

# *Clues on interstellar magnetized turbulence from Planck observations*

François LEVRIER



Laboratoire d'Étude du Rayonnement et de la Matière en Astrophysique

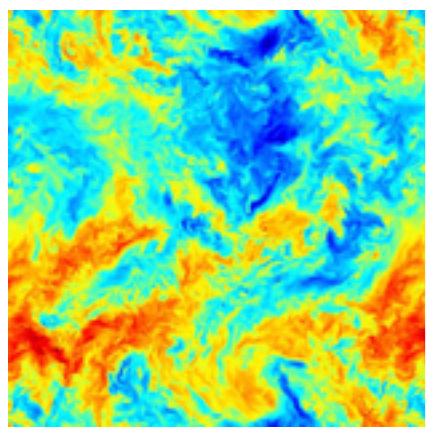
# Talk outline

- **Lightning-fast introduction...**
- **Planck thermal dust polarization and MHD turbulence**
- **Current work (also talk by F. Boulanger)**

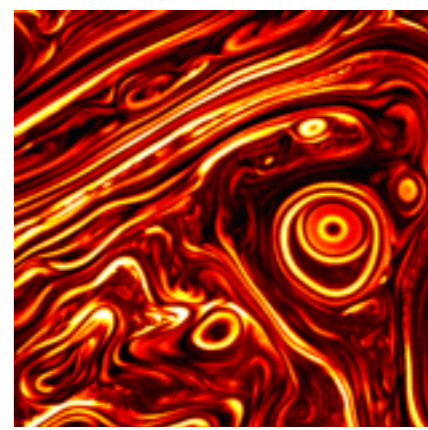
# Turbulence

« *Big whirls have little whirls that feed on their velocity, and little whirls have lesser whirls and so on to viscosity.* »

Lewis Fry Richardson (1920)

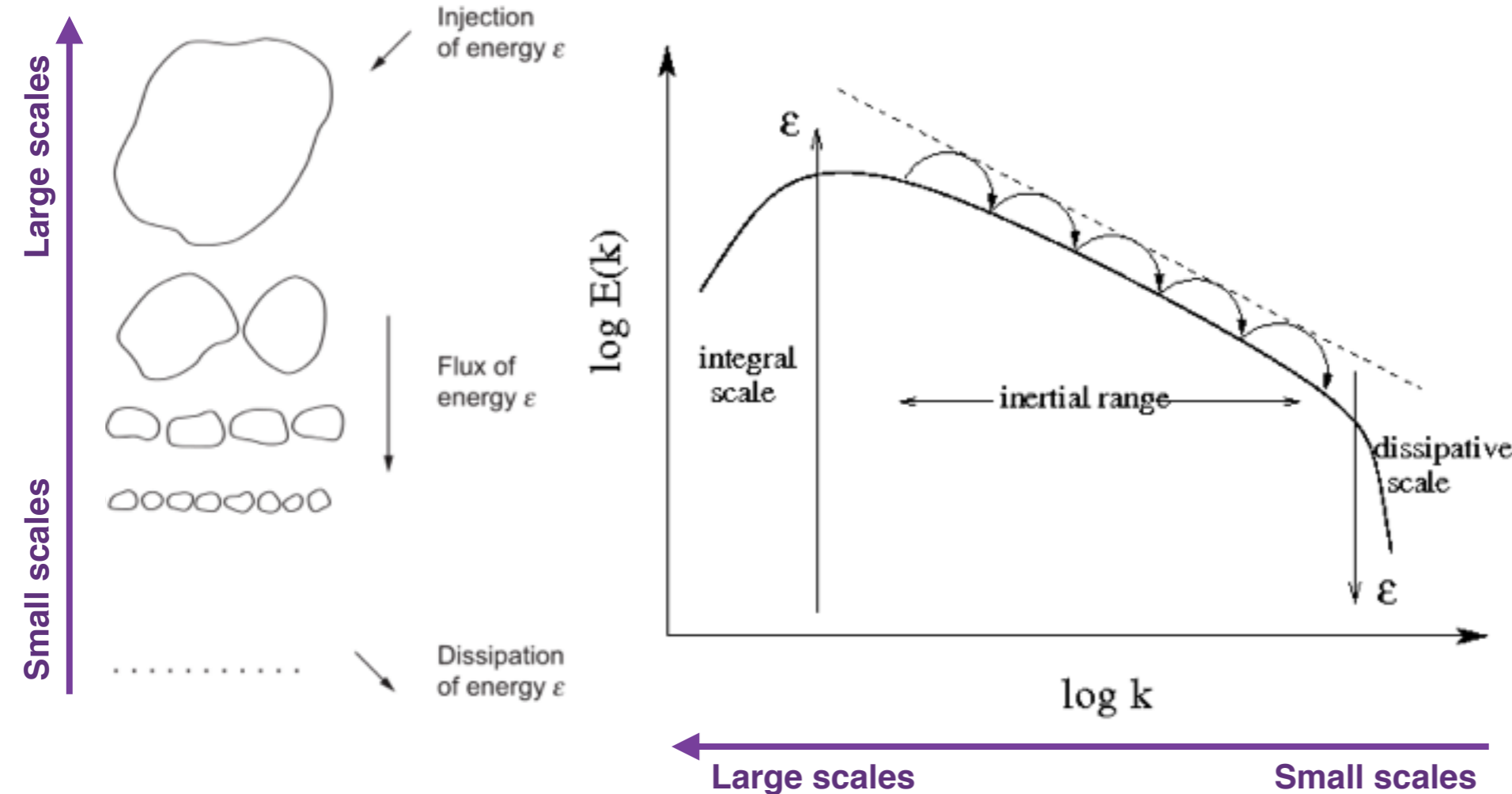


Vorticity (JHU)



Current (UCSD, Berkeley Lab)

- Kolmogorov's K41 theory for HD turbulence : incompressible, homogeneous, isotropic cascade
- Scaling laws and self-similarity
- Intermittency : dissipation of energy occurs in bursts, localized in time and space
- Modification of scaling laws from compressibility and magnetic fields (MHD turbulence)



**Kolmogorov 1941**

$$P_v(k) \propto \epsilon^{2/3} k^{-5/3}$$

**Iroshnikov 1964, Kraichnan 1965**

$$P_v(k) \propto (\epsilon v_A)^{1/2} k^{-3/2}$$

**Sridhar & Goldreich 1994, 1995**

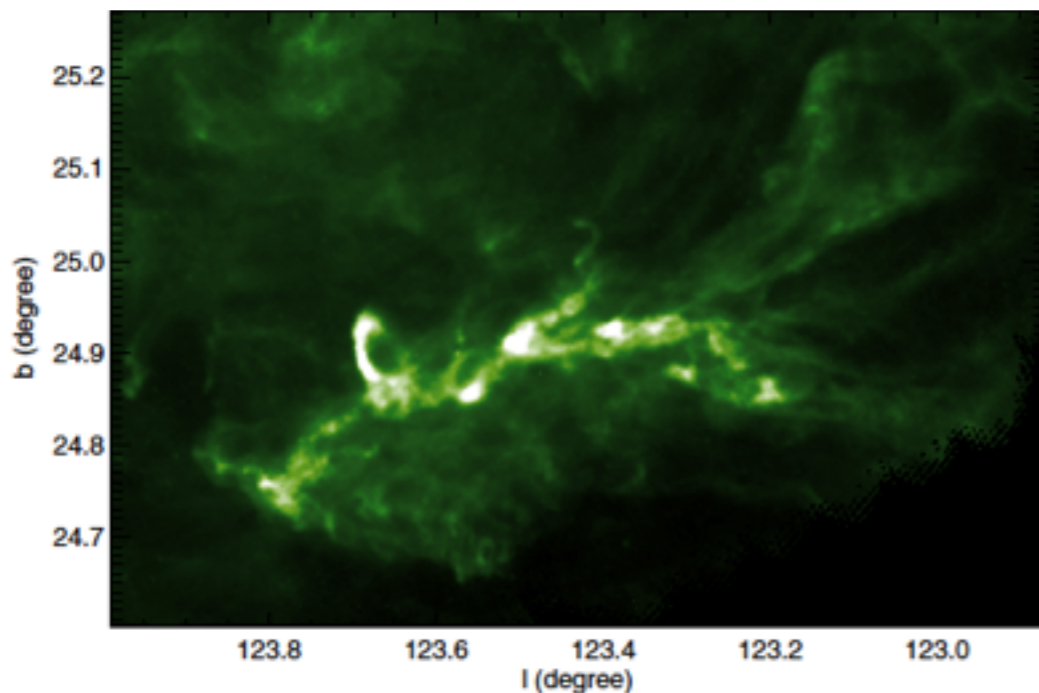
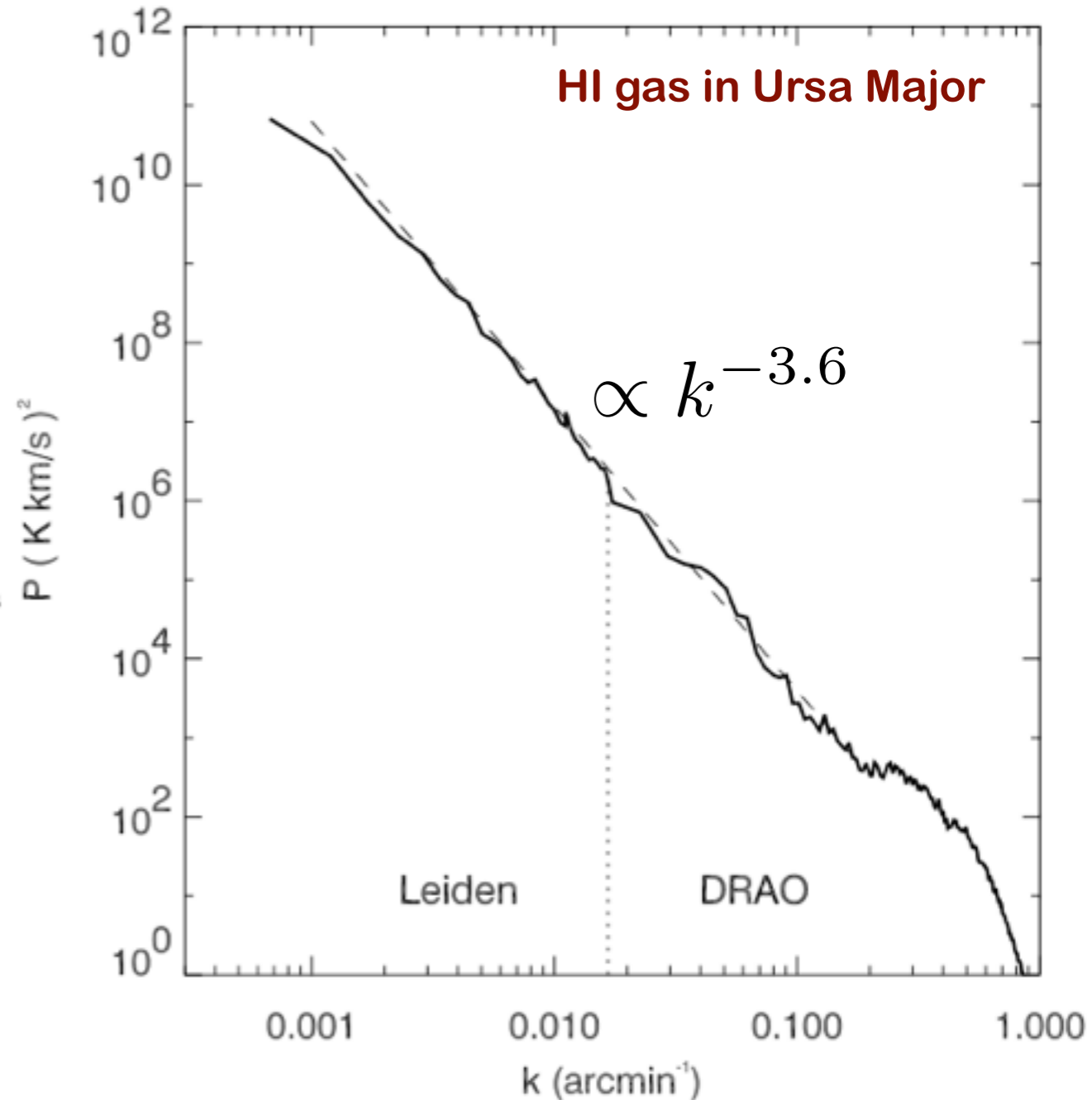
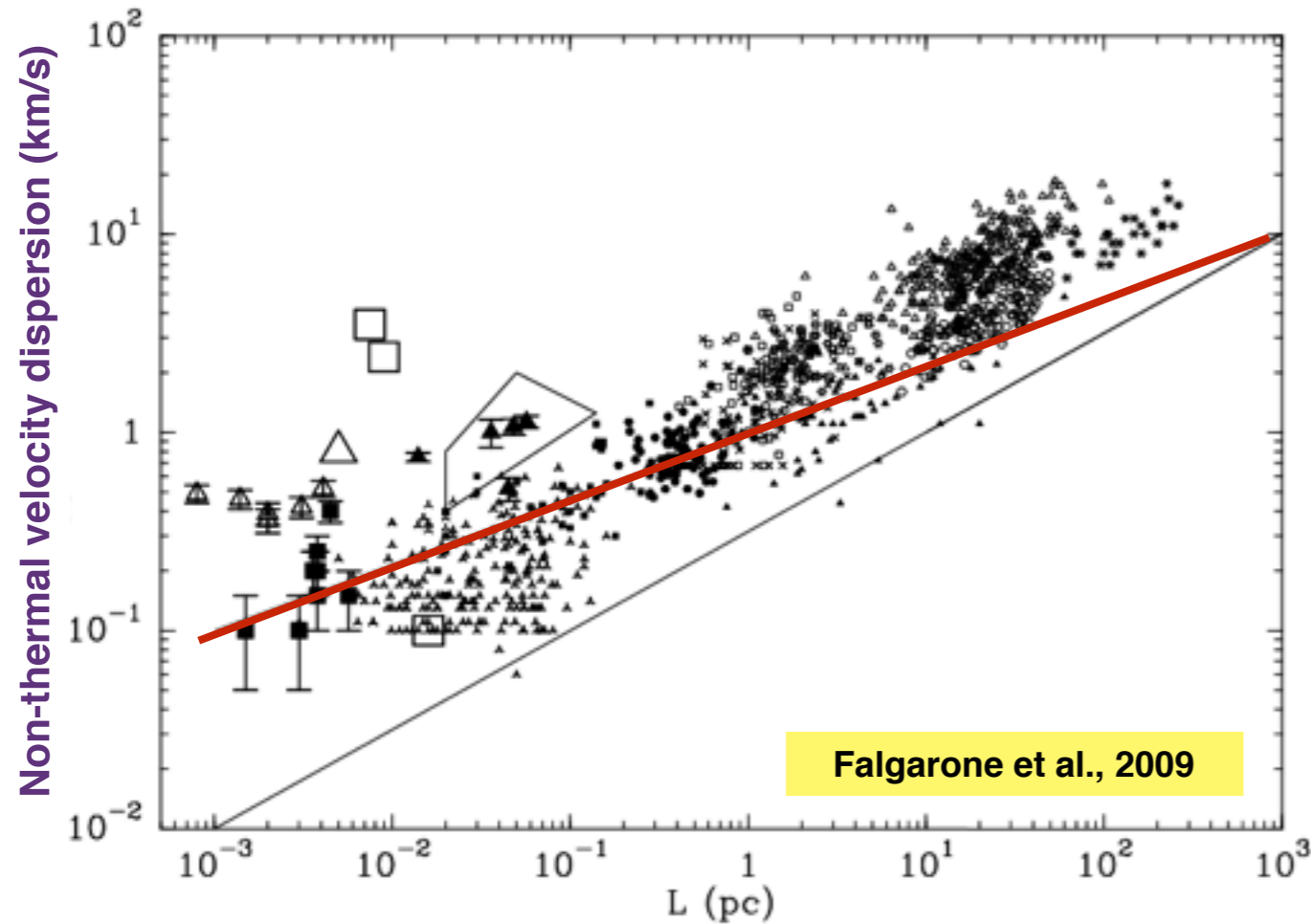
$$P_{v_\perp}(k) \propto k_\perp^{-5/3}$$

**Kowal & Lazarian 2007**

$$P_{\rho^{1/3}v}(k) \propto k^{-5/3}$$

# Turbulence in the ISM

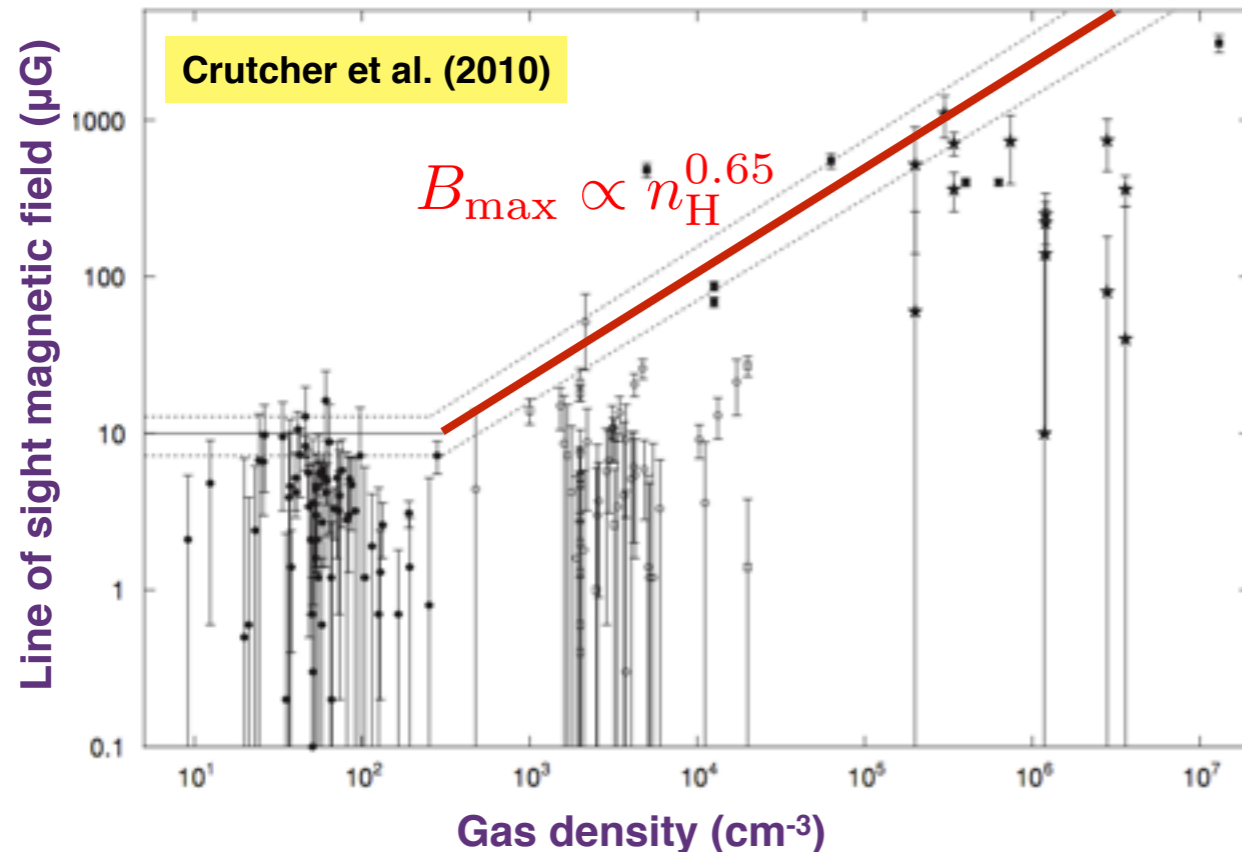
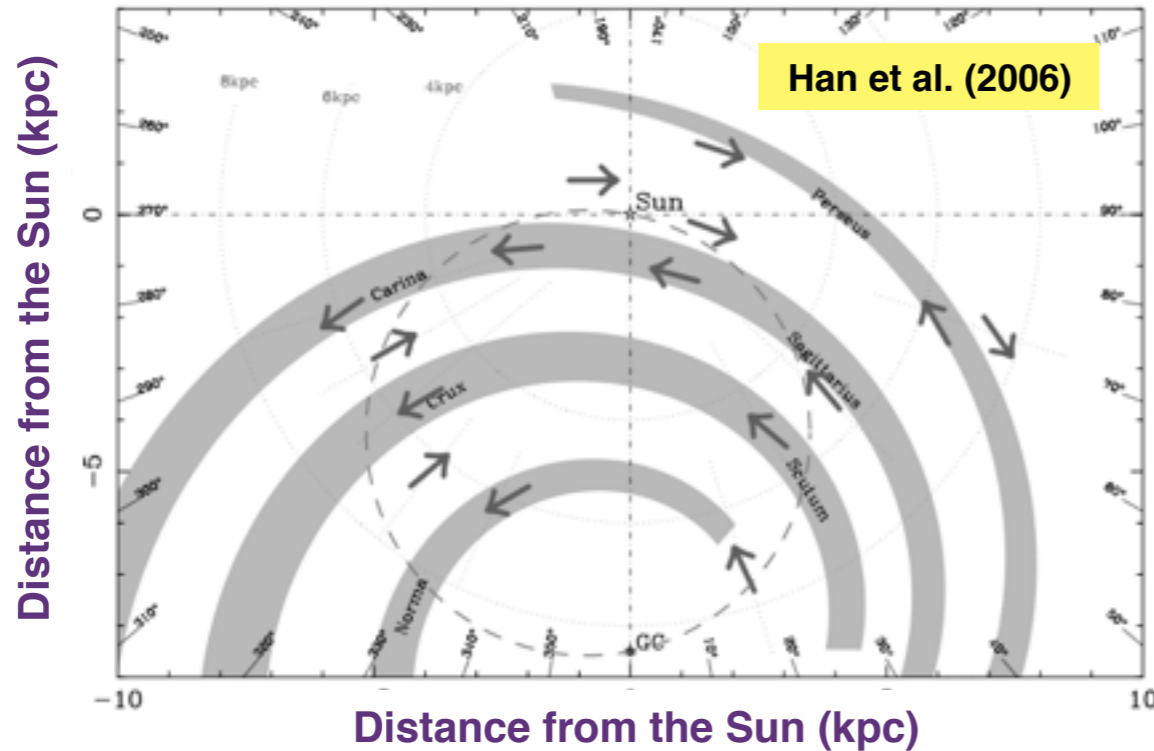
- Suprathermal linewidths, scaling with the size of structures
- Self-similarity of structures across many scales
- Intermittency at small scales : non-Gaussian wings in distributions of centroid velocity increments



# Magnetic fields in the Milky Way

- Coupled to the gas, provides balance with gravity, controls the propagation of cosmic rays
- Generated from primordial seed fields via a coupling of differential rotation and Coriolis force
- Superposition of a large-scale field following spiral arms and of a turbulent component

## Field reversals



$$B = B_0 + B_t$$

$\sim$  a few  $\mu\text{G}$        $\sim$  a few  $\mu\text{G}$

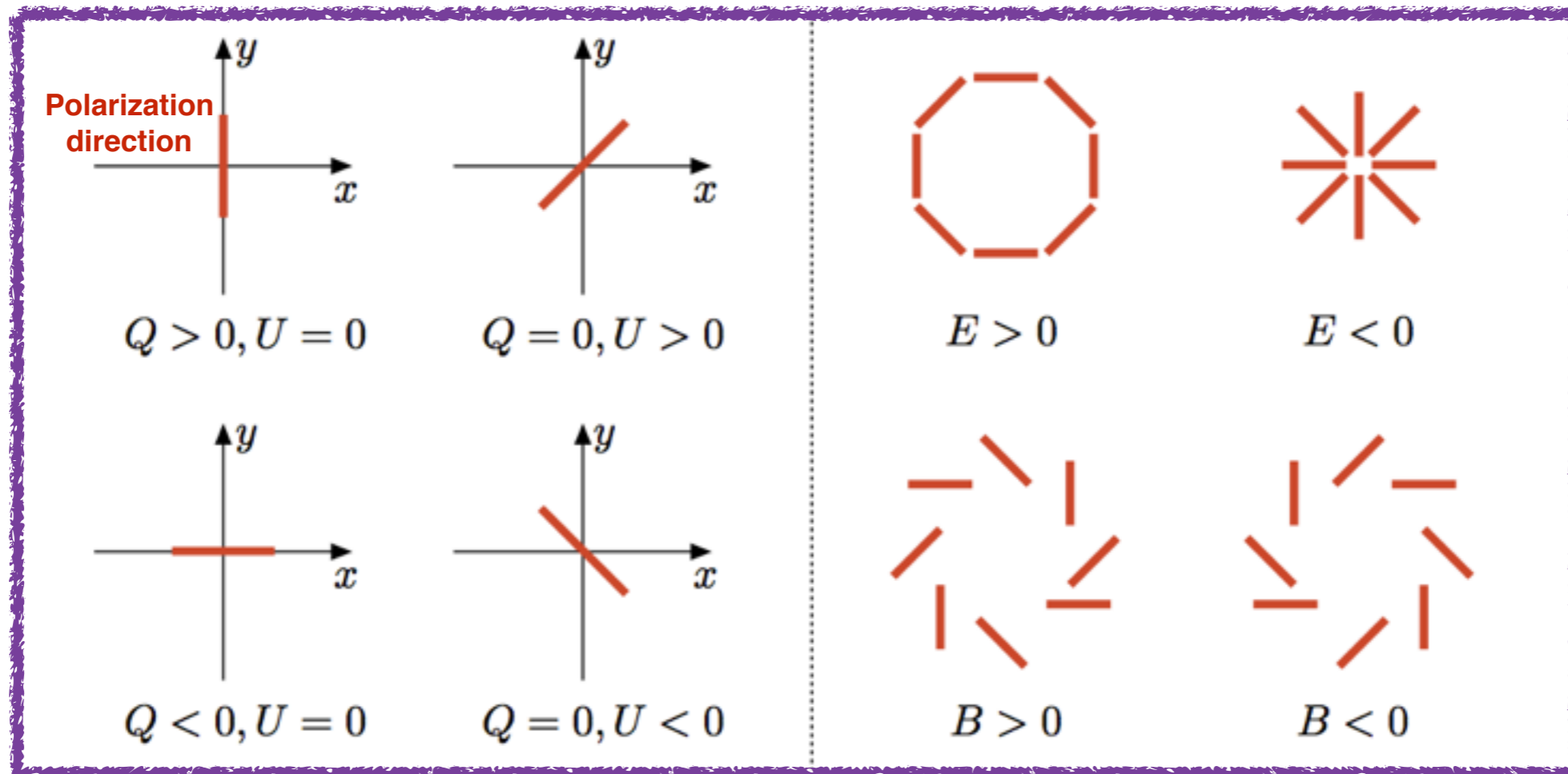
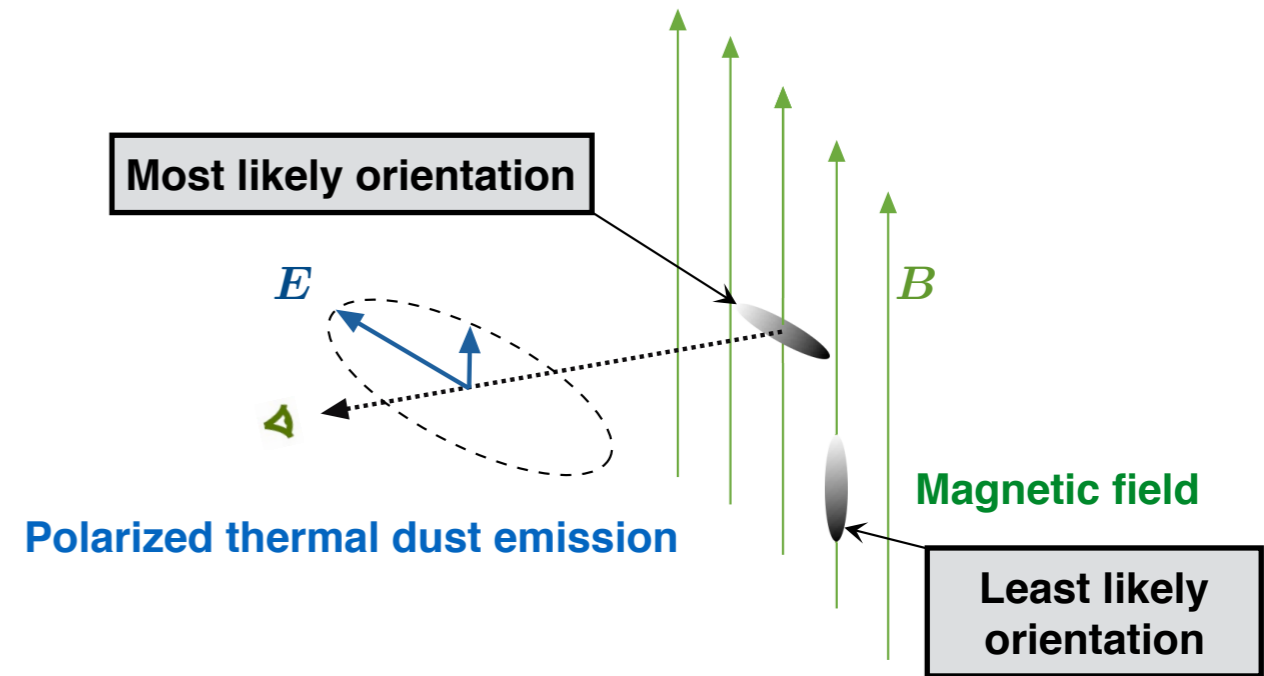
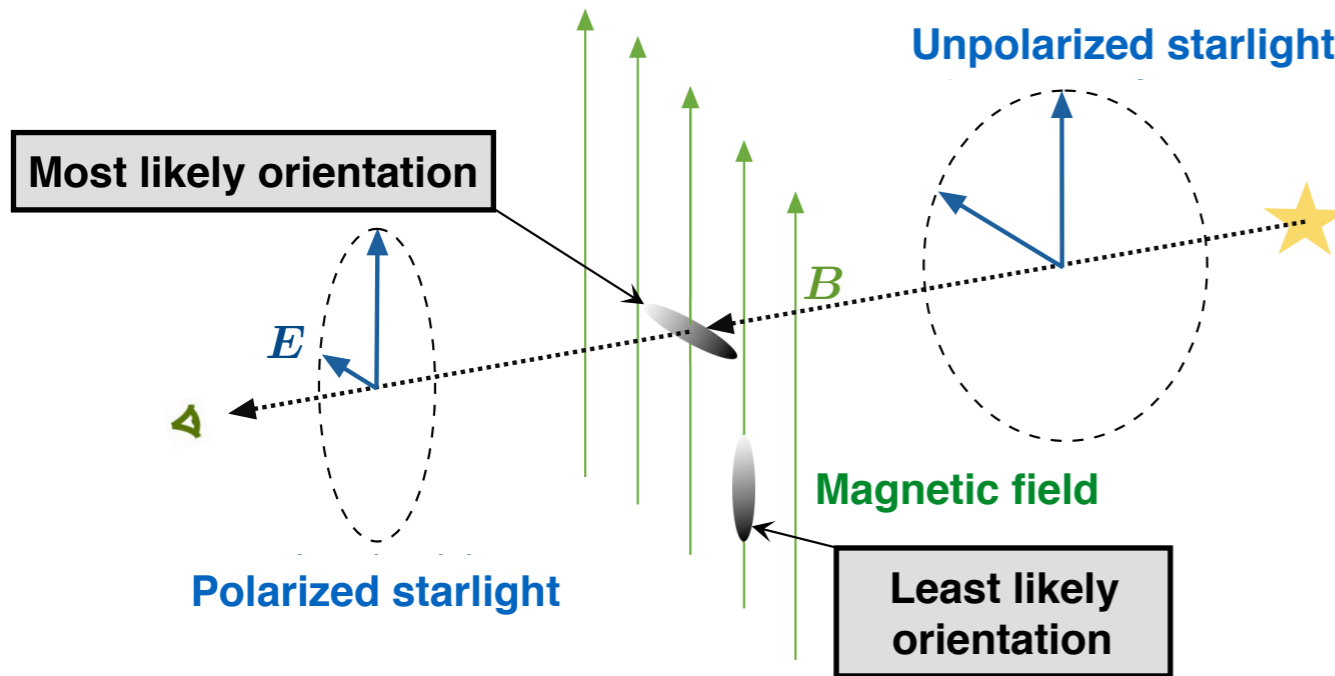
Haverkorn et al. (2008)

## Measurement methods

Notation	Observational signatures
$B_{\text{tot},\perp}^2 = B_{\text{turb},\perp}^2 + B_{\text{reg},\perp}^2$	Total synchrotron intensity
$B_{\text{turb},\perp}^2 = B_{\text{iso},\perp}^2 + B_{\text{aniso},\perp}^2$	Total synchrotron emission, partly polarized
$B_{\text{iso},\perp}$ ( $= \sqrt{2/3} B_{\text{iso}}$ )	Unpolarized synchr. intensity, beam depolarization, Faraday depolarization
$B_{\text{iso},\parallel}$ ( $= \sqrt{1/3} B_{\text{iso}}$ )	Faraday depolarization
$B_{\text{ord},\perp}^2 = B_{\text{aniso},\perp}^2 + B_{\text{reg},\perp}^2$	Intensity and vectors of radio, optical, IR & submm pol.
$B_{\text{aniso},\perp}$	Intensity and vectors of radio, optical, IR & submm pol., Faraday depolarization
$B_{\text{reg},\perp}$	Intensity and vectors of radio, optical, IR & submm pol., Goldreich-Kylafis effect
$B_{\text{reg},\parallel}$	Faraday rotation + depol., longitudinal Zeeman effect

# Dust, magnetic fields and polarization

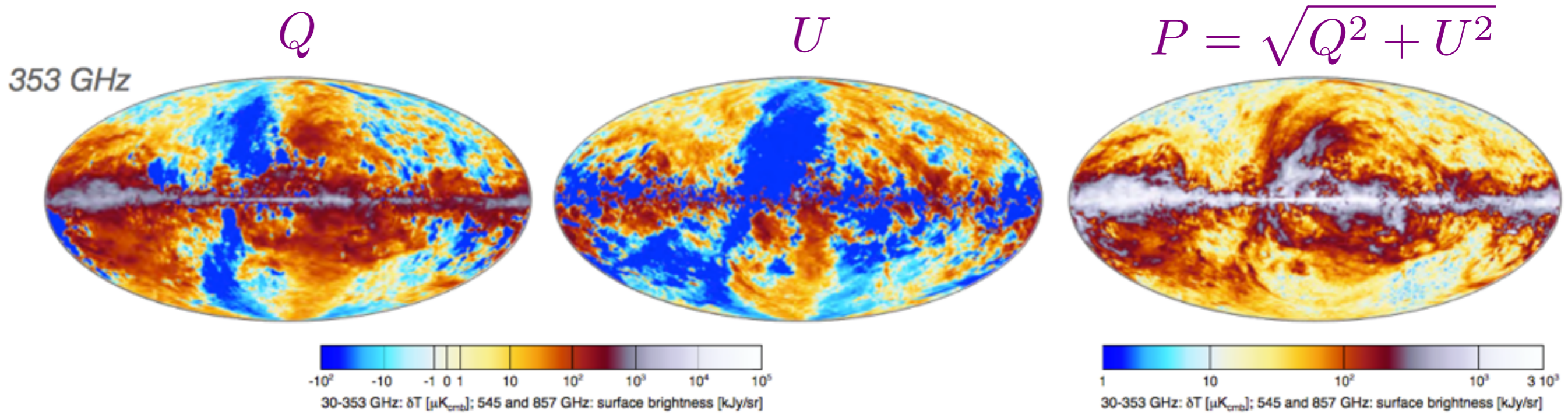
- Aspherical, charged, rotating dust grains statistically align in the local magnetic field
- Background starlight emerges polarized parallel to the magnetic field
- Polarized thermal dust emission arises perpendicularly to the magnetic field



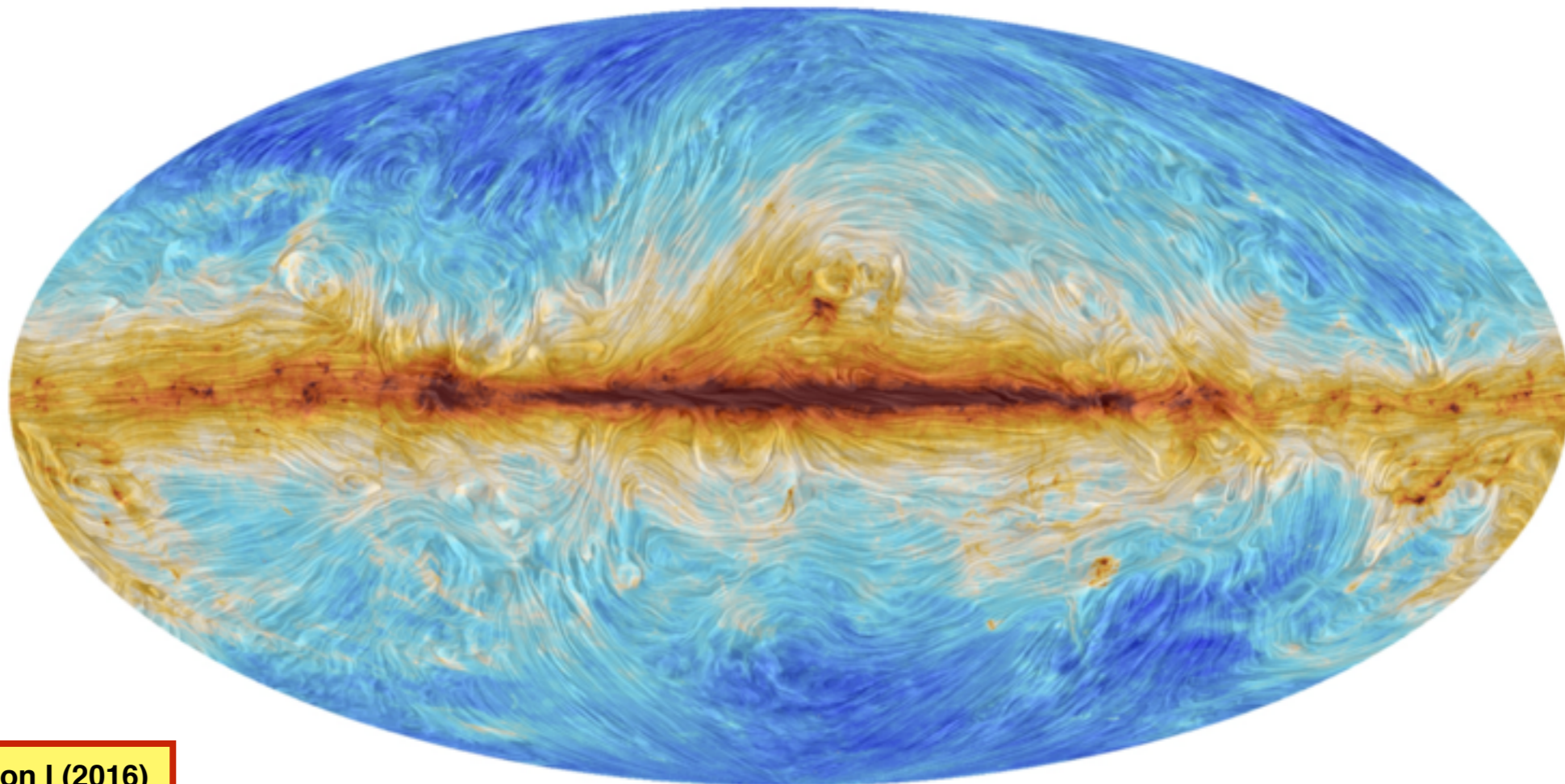
Stokes Parameters

E- and B-modes

# The Planck view of the Galactic magnetic field



Total intensity and « drapery » showing the direction of the magnetic field

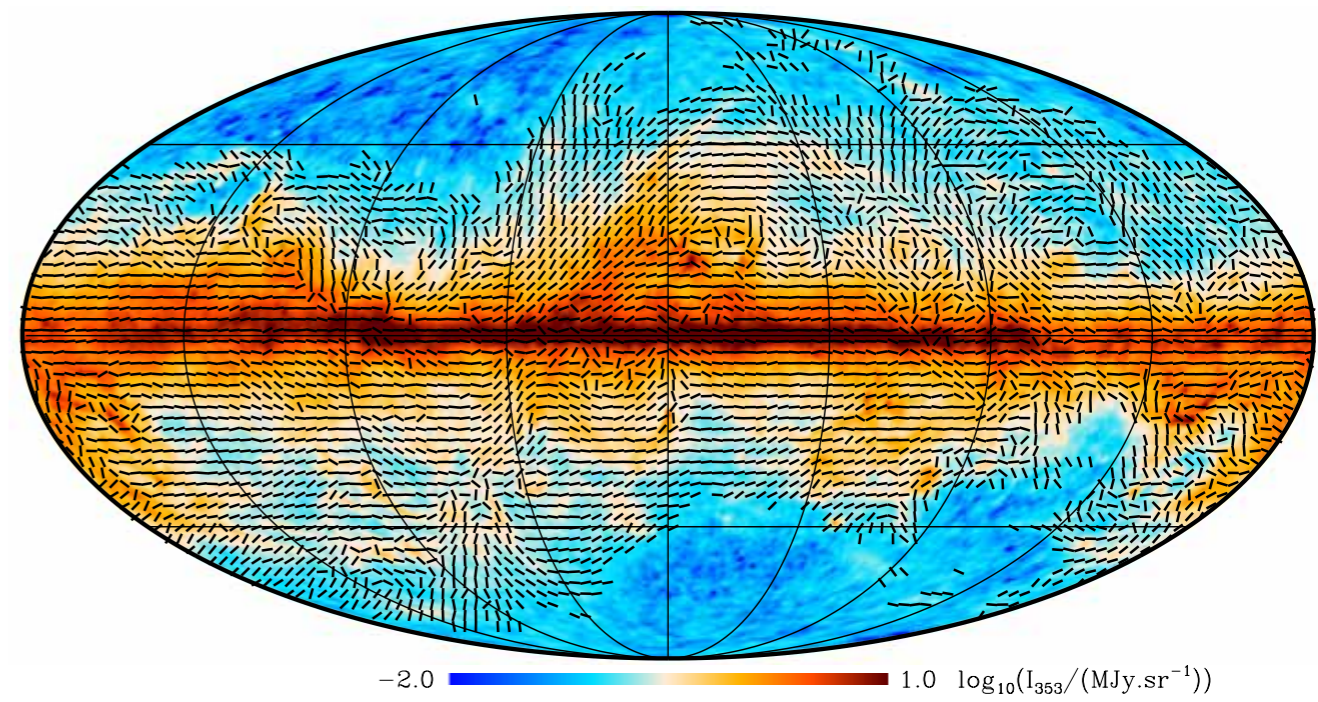
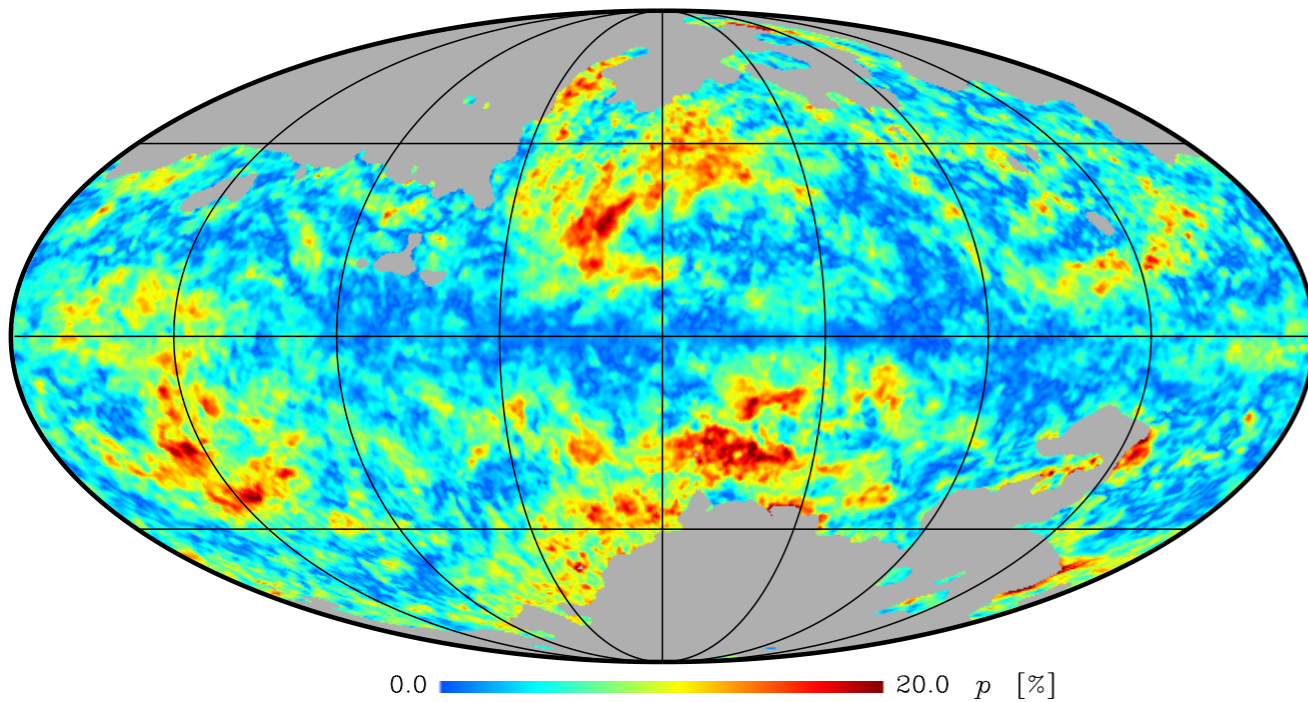


# Properties of large-scale thermal dust polarization

- Low polarization fractions in the Galactic Plane and some highly polarized regions
- Thin filamentary structures of low polarization with no material counterpart

Polarization fraction  $p = \frac{P}{I}$

Polarization angle  $\psi = \frac{1}{2} \text{atan}(U, Q)$



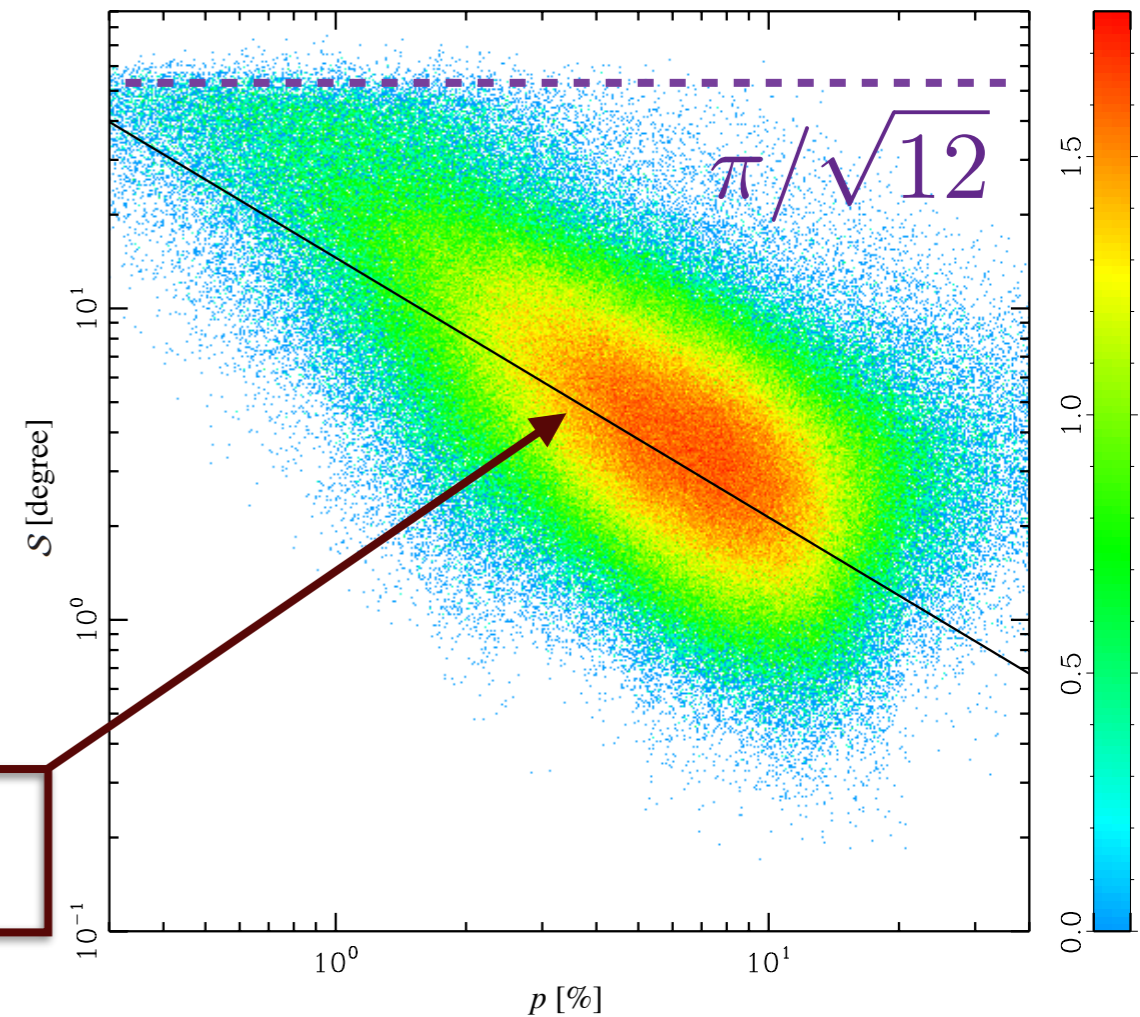
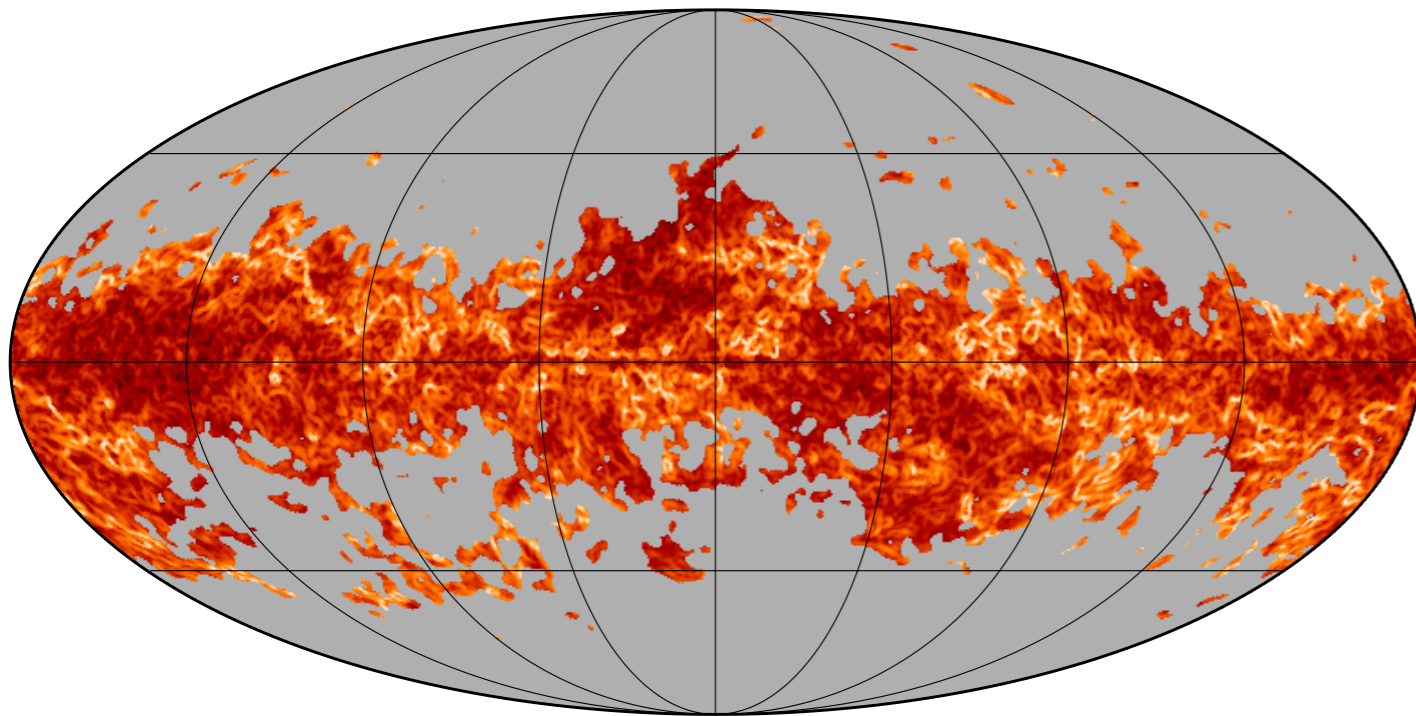
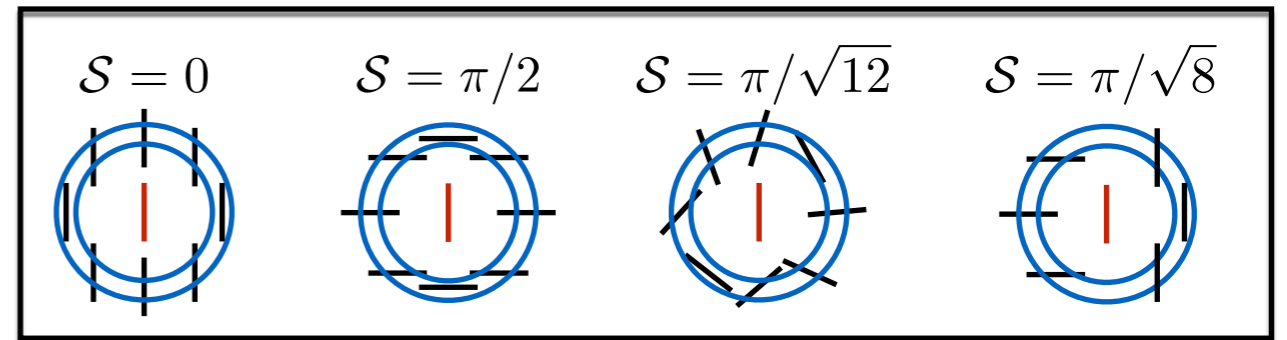
Update in early 2017...



# Spatial structure of the polarization angle map

## Polarization angle dispersion function

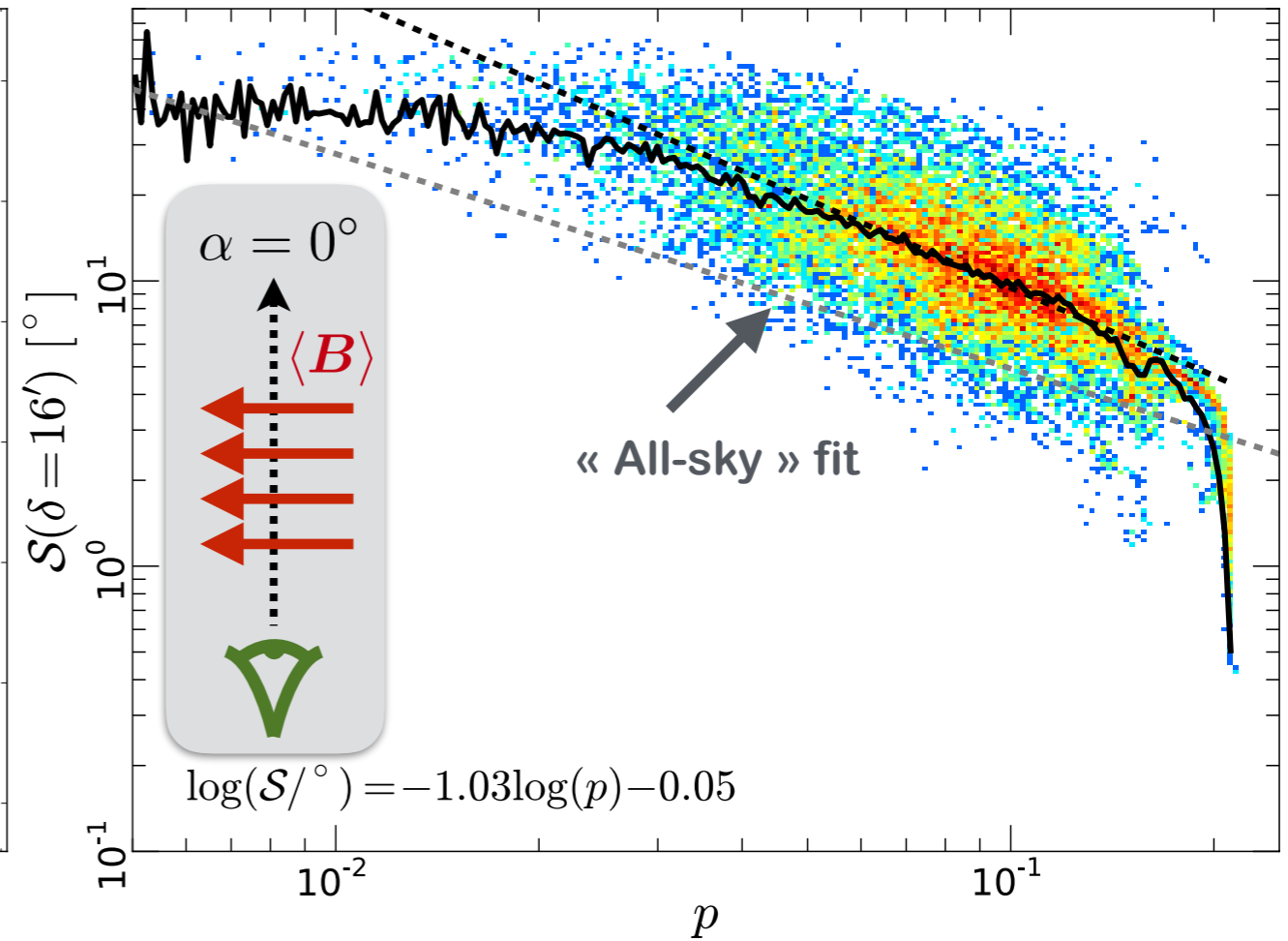
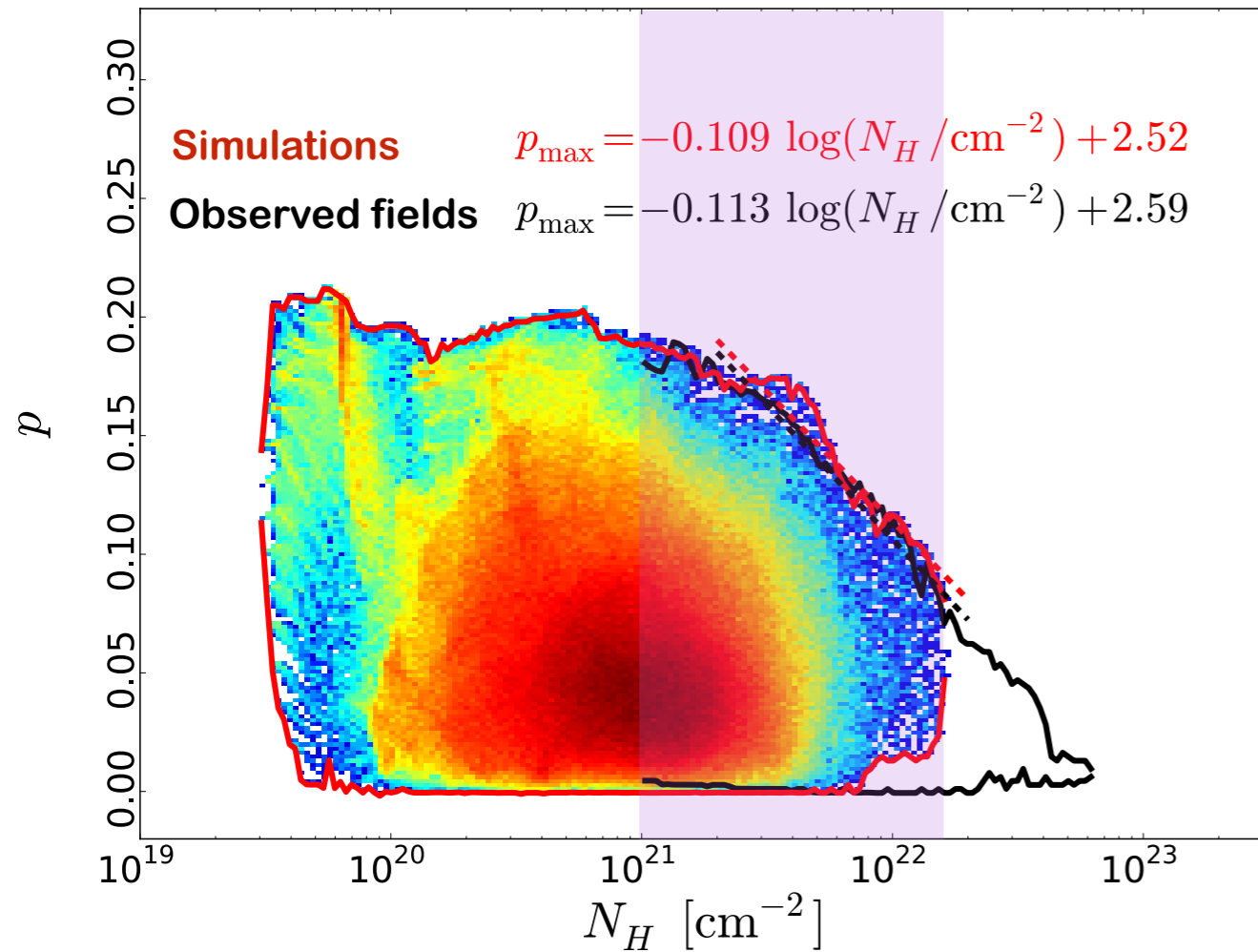
$$\mathcal{S}(\mathbf{r}, \delta) = \sqrt{\frac{1}{N} \sum_{i=1}^N [\psi(\mathbf{r} + \delta_i) - \psi(\mathbf{r})]^2}$$



$$\log(\mathcal{S} / \text{deg}) = -0.834 \log p - 0.504$$

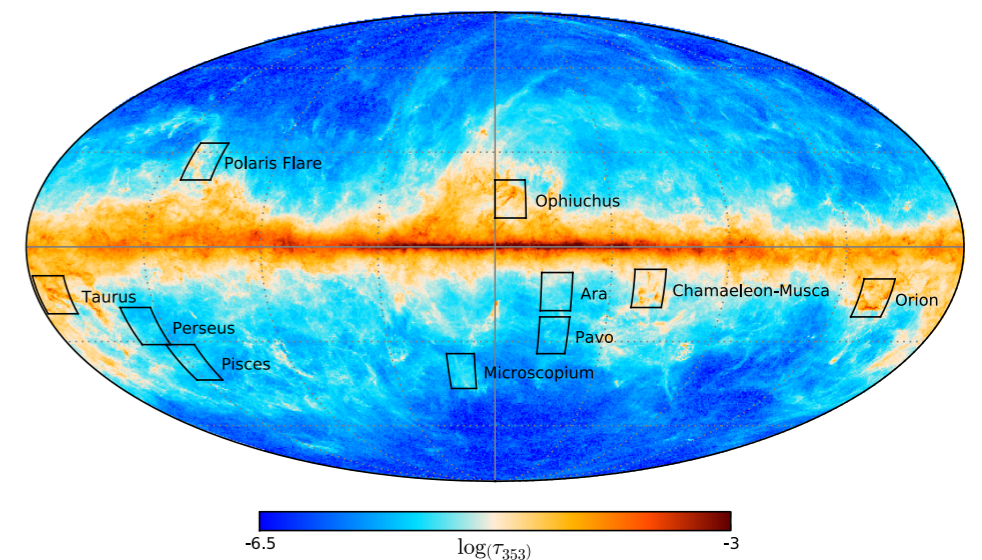
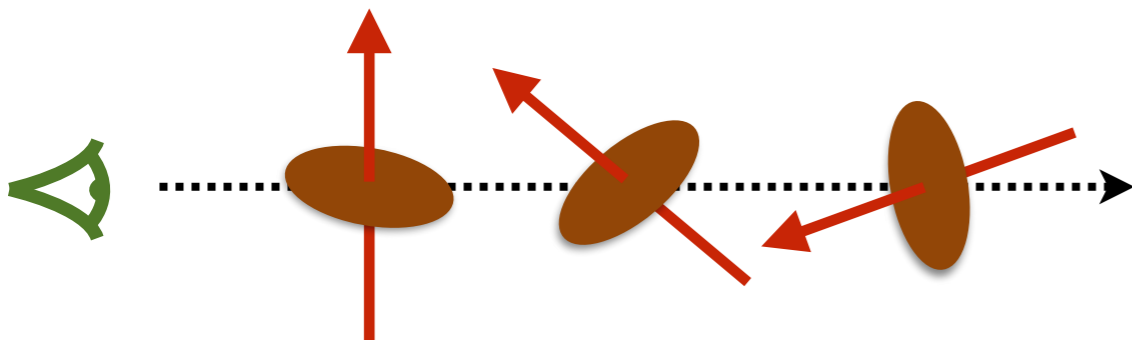
- Strongly anti-correlated with the polarization fraction
- Low polarization fractions found where the polarization angle direction changes abruptly
- Increased lag  $\delta$  flattens the anti-correlation

# Comparison with a simulation of anisotropic MHD turbulence



- Simulations reproduce the decrease of the maximum polarization fraction with  $N_H$  in that range
- The global anti-correlation with the polarization angle dispersion function is reproduced, with a shift

An effect of magnetic field tangling on the line of sight...

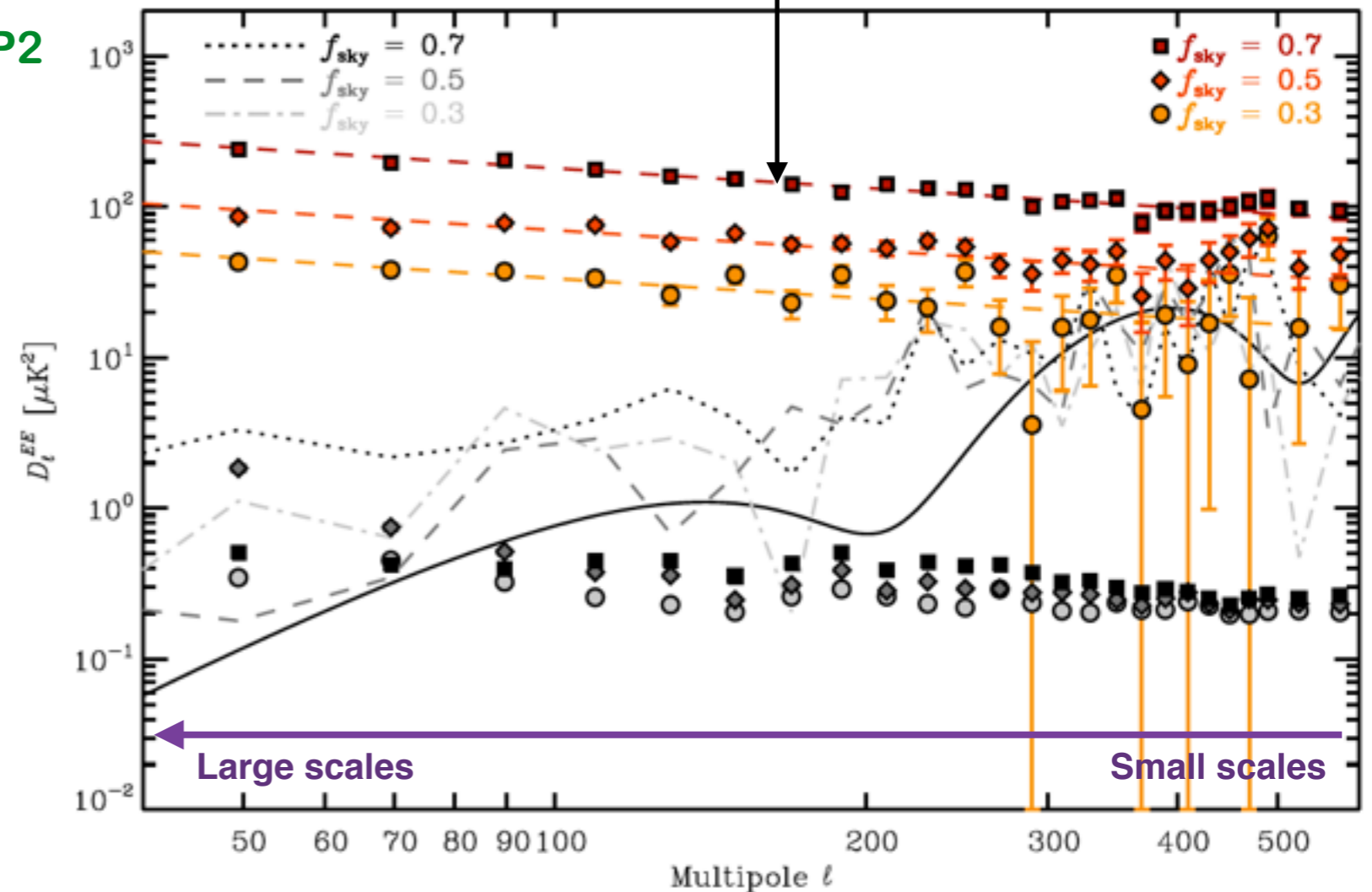
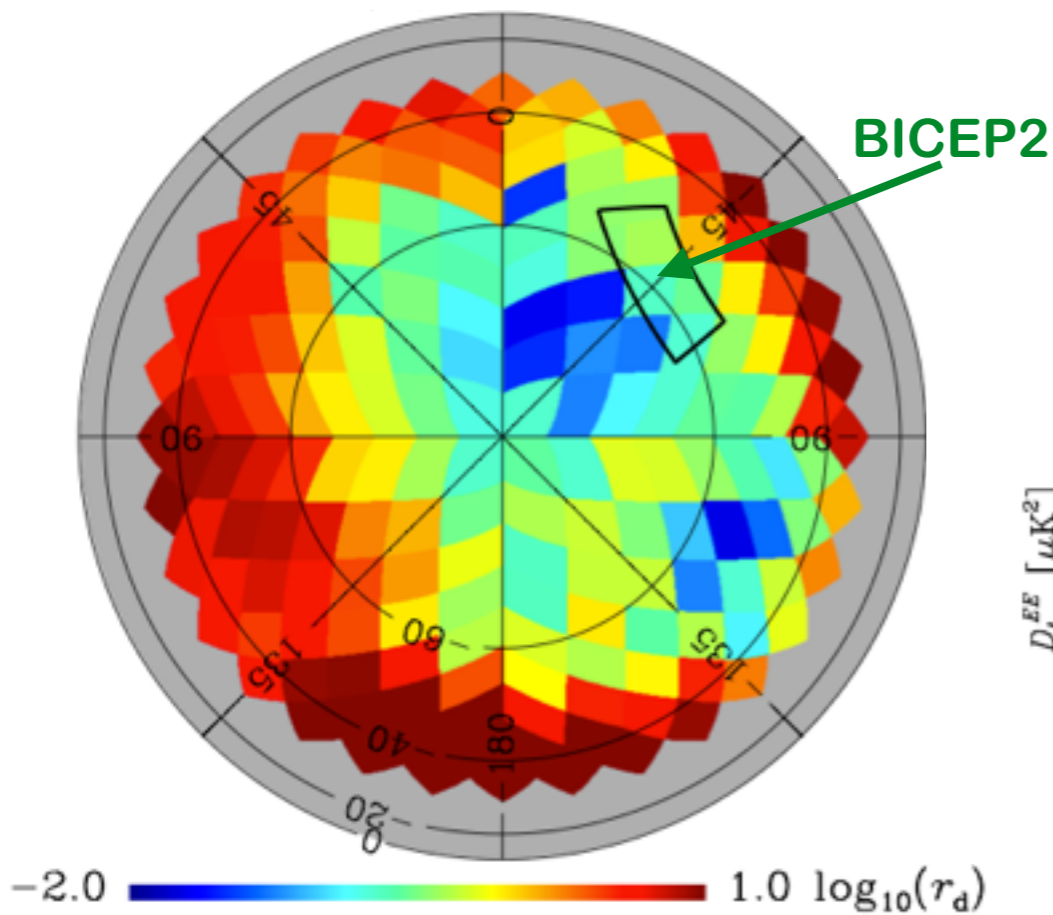


# The angular power spectrum of polarized thermal dust emission

- E and B thermal dust emission angular power spectra outside the Galactic plane well fit by power laws
- B mode power attributable to dust in the BICEP2 field compatible with reported detection

BICEP2 Collaboration (2014)

$$D_\ell = \frac{\ell(\ell + 1)}{2\pi} C_\ell$$



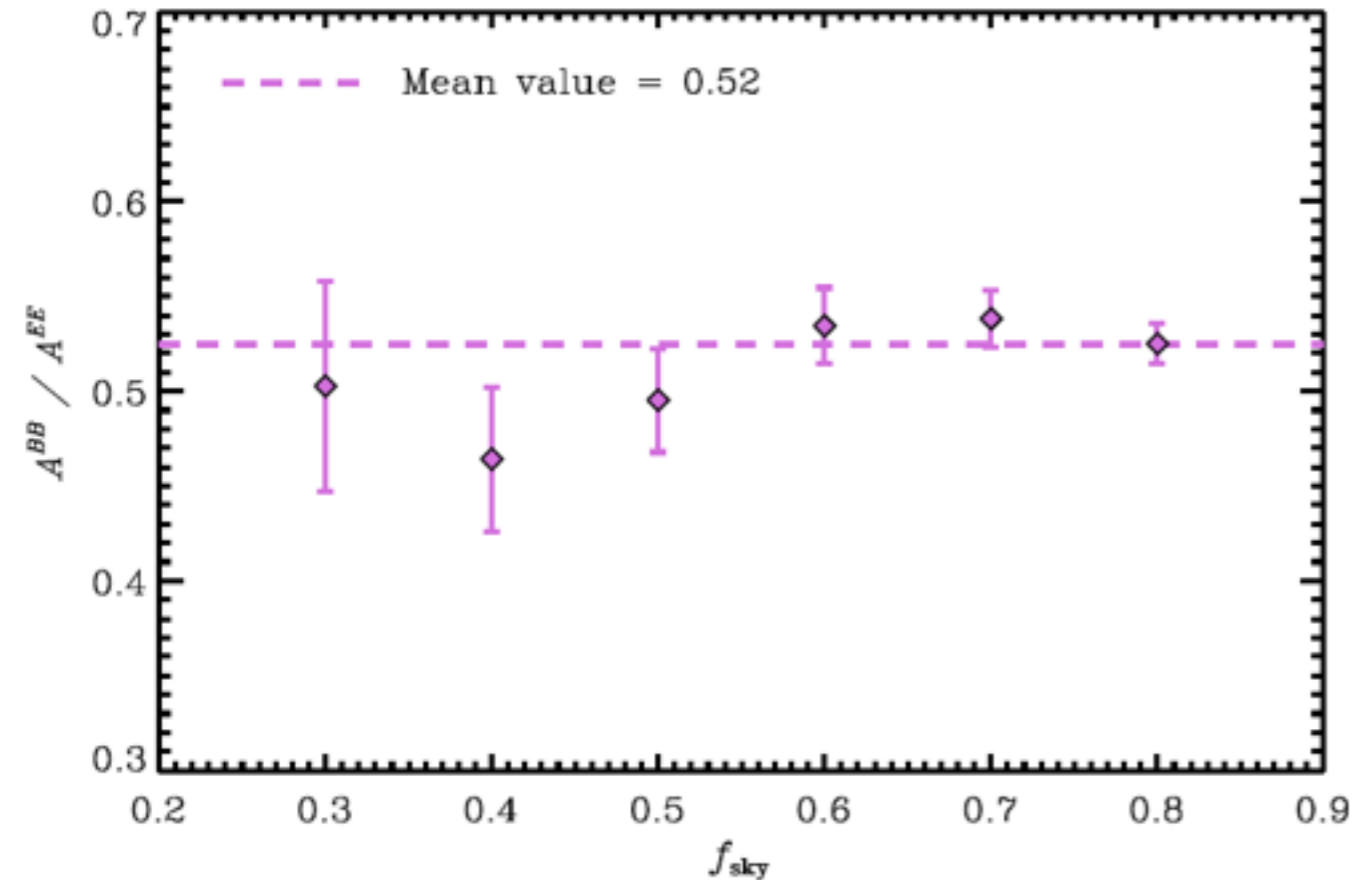
$$C_\ell^{EE} \propto \ell^{\alpha_{EE}} \quad C_\ell^{BB} \propto \ell^{\alpha_{BB}}$$

$$\alpha_{EE, BB} = -2.42 \pm 0.02$$

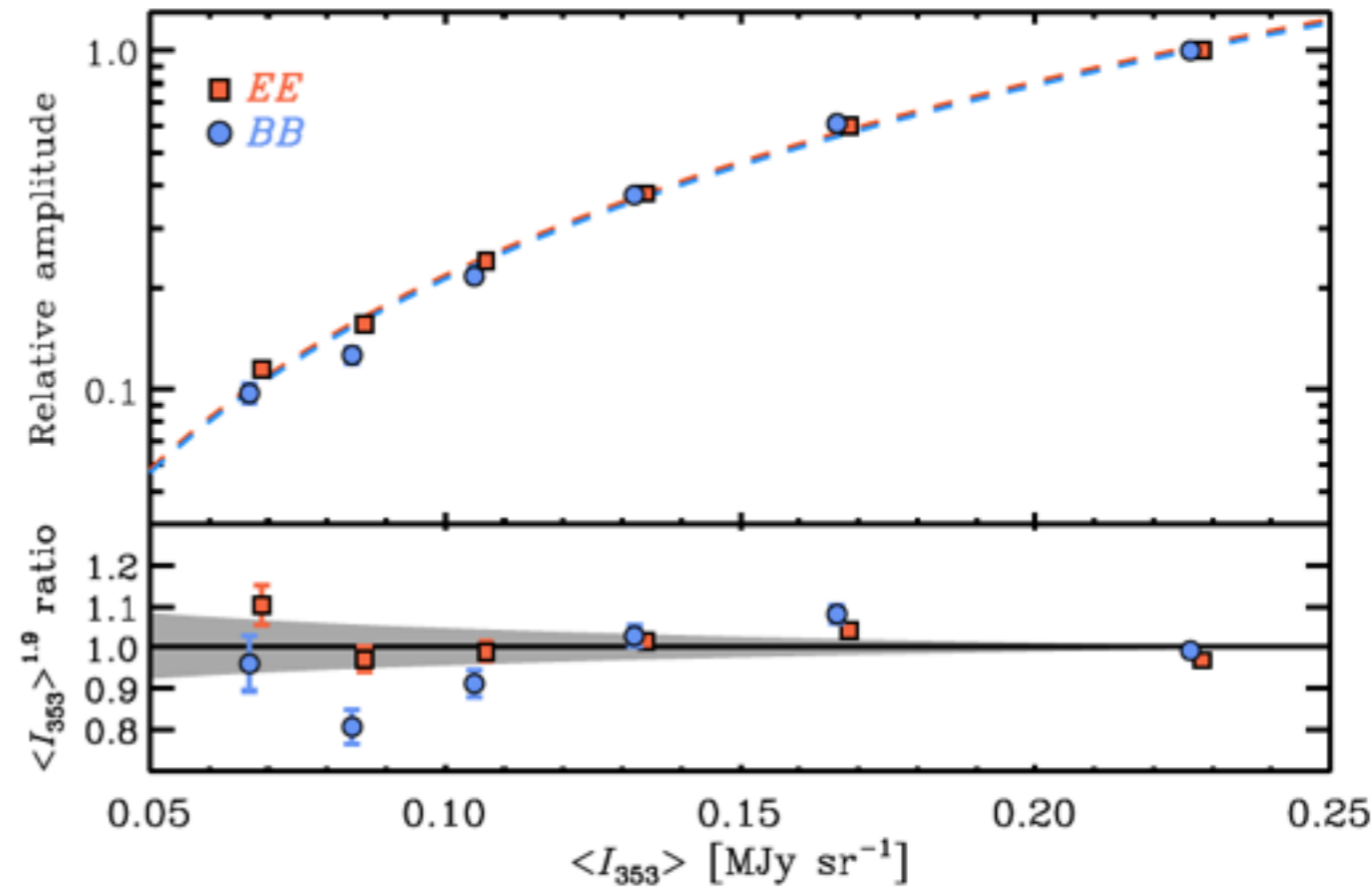
# The angular power spectrum of polarized thermal dust emission

- Amplitudes vary approximately as the square of average dust brightness in the selected region
- Asymmetry in the E and B modes : twice as much power in E modes

### B/E asymmetry

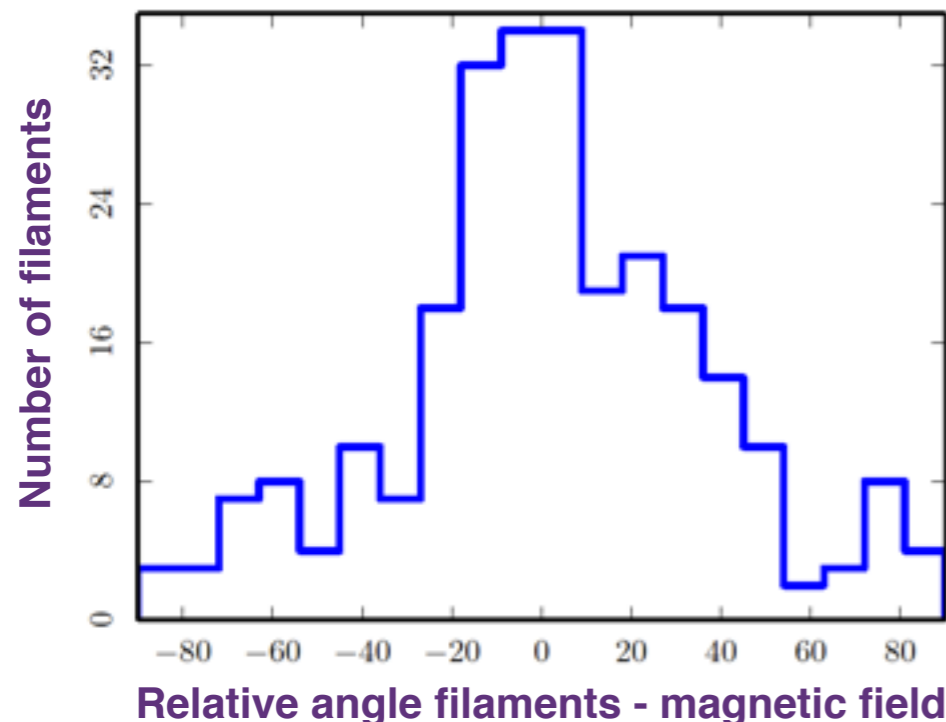
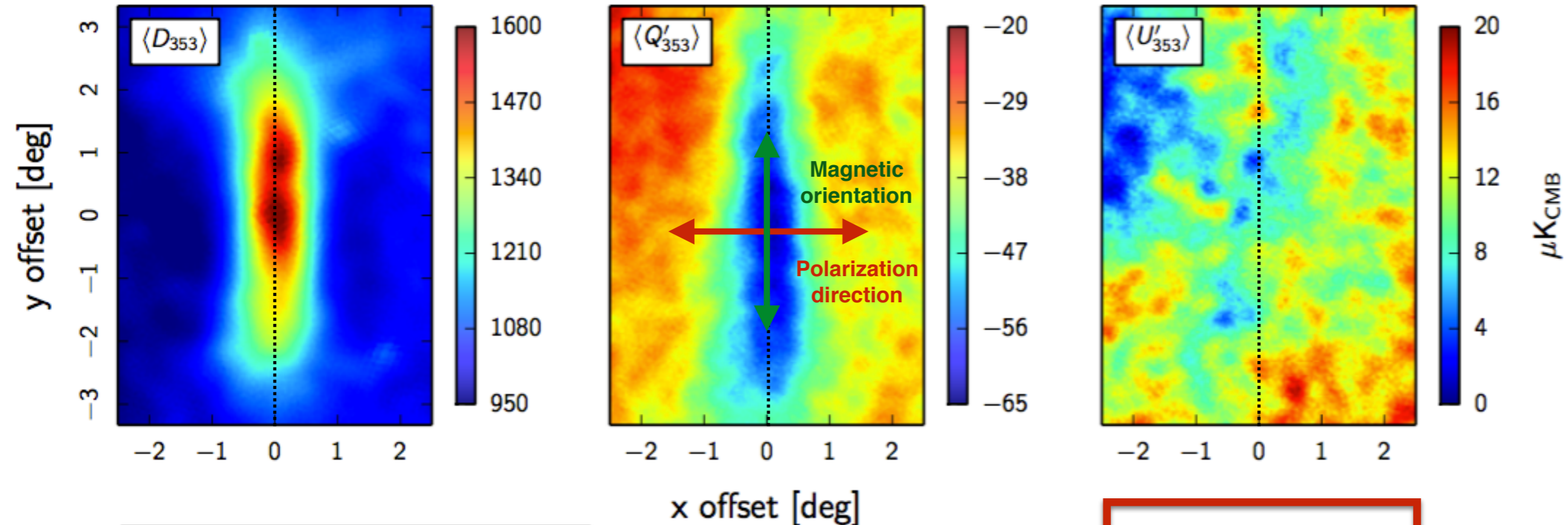


### Scaling with dust emission intensity



# Origin of the E/B power asymmetry

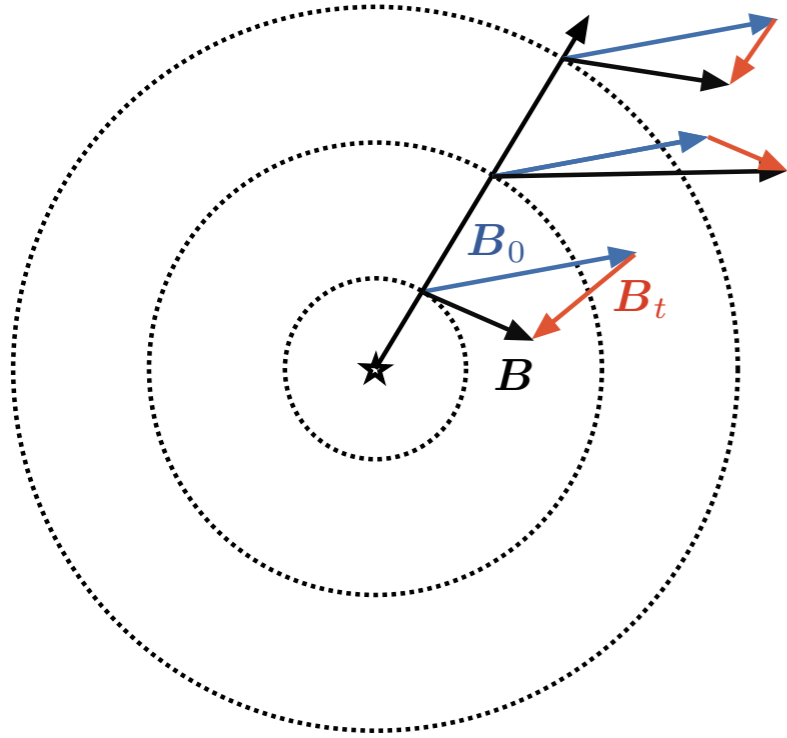
- Identification of 259 matter filaments longer than  $2^\circ$  in the high Galactic latitude sky using the Hessian
- Preferential alignment of the filaments with the magnetic field
- Stacking of Stokes parameter maps rotated along the filaments leads to mean polarization fraction
- E/B asymmetry may be accounted for by this preferential alignment



$$\langle p \rangle = 11\%$$

$$\frac{A^{BB}}{A^{EE}} \simeq \frac{\langle \sin^2 2\Delta_{\bar{\chi}-\bar{\theta}_-}^F \rangle}{\langle \cos^2 2\Delta_{\bar{\chi}-\bar{\theta}_-}^F \rangle} = 0.66$$

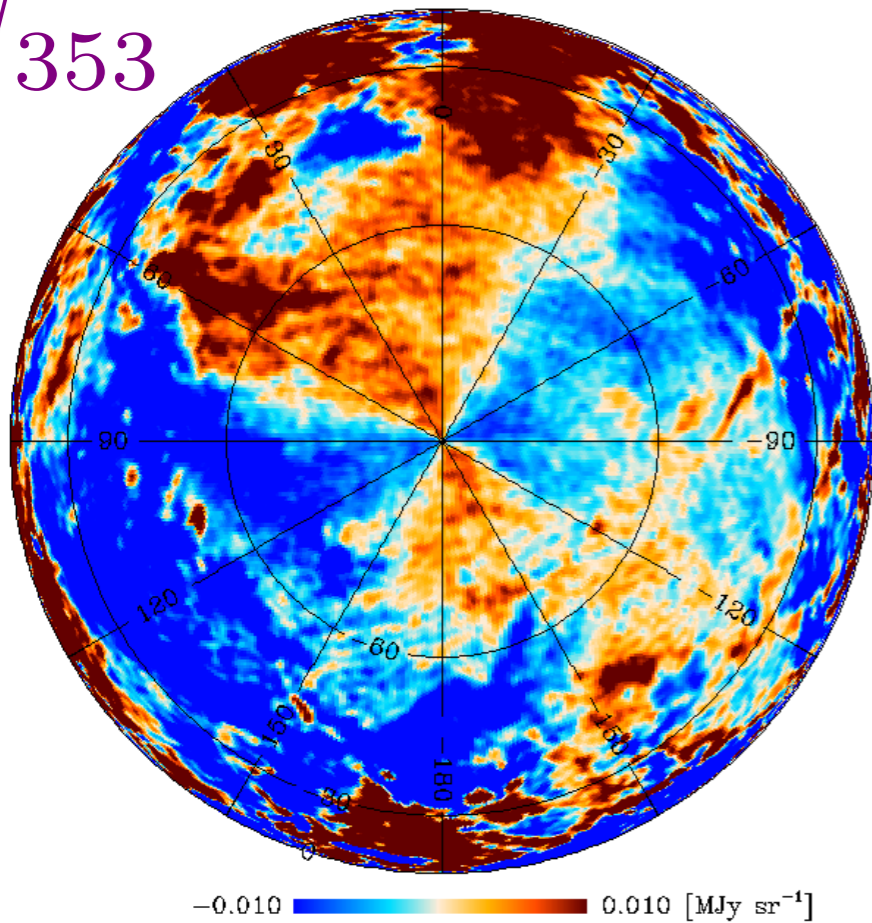
# A Gaussian model of the polarized sky



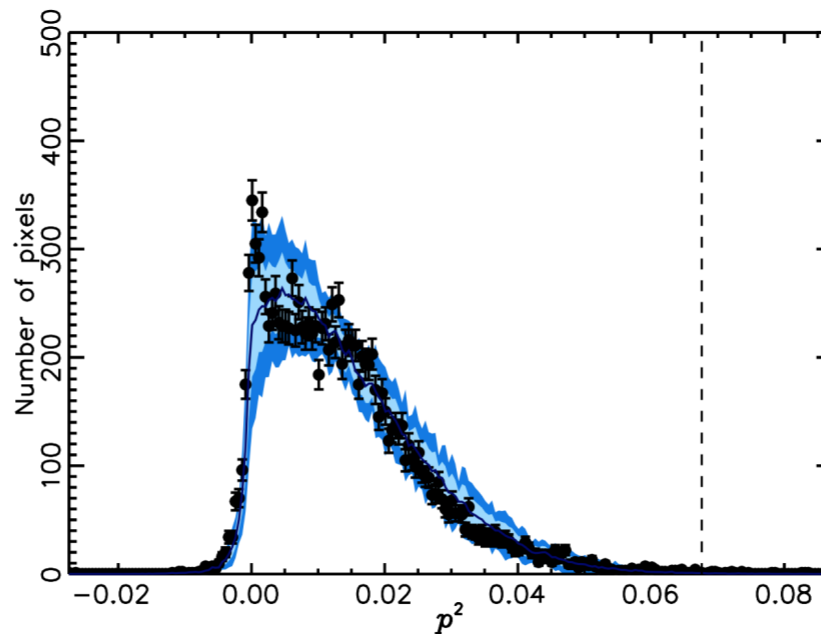
Magnetic field  $B = B_0 + B_t$   
 Uniform field Uniform field Turbulent field

- A superposition of variously polarized layers (turbulent cells ?)
- Turbulent field : 3D Gaussian random variable
- Analysis of the Southern Galactic cap
  - Spatial power spectrum unconstrained  $C_\ell \propto \ell^{\alpha_M}$
  - Direction of the large-scale field  $(l_0, b_0) = (70 \pm 5^\circ, 24 \pm 5^\circ)$
  - Turbulent-to-mean ratio  $f_M = 0.9 \pm 0.1$
  - Number of layers  $N = 7 \pm 2$
  - Intrinsic polarization fraction  $p_0 = 26 \pm 3\%$

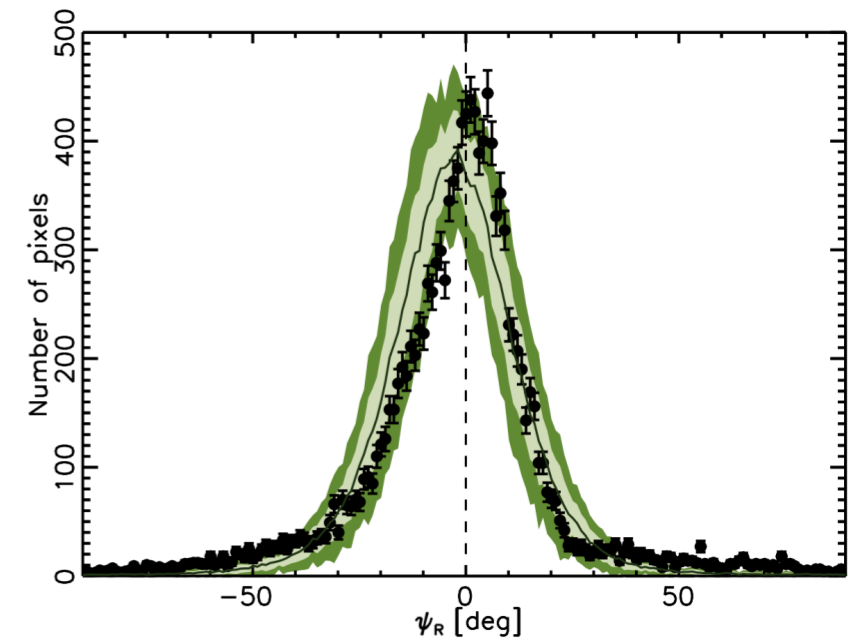
$U_{353}$



Observations (black dots) vs. Simulations (colored regions)



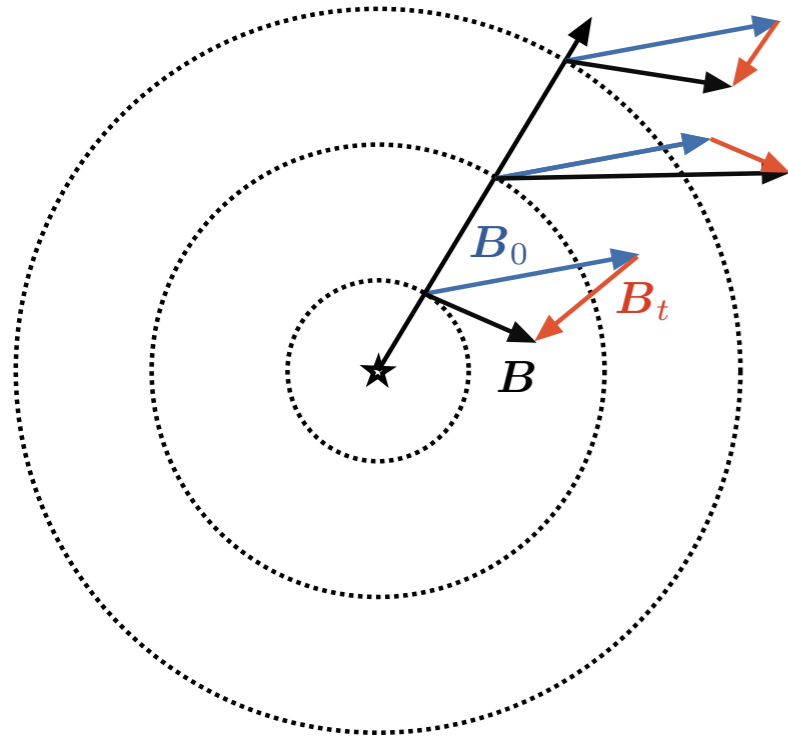
Polarization fraction



Polarization angle relative to the large-scale field

# Perspectives on modelling polarized thermal dust emission

- Stacking of a small number of polarized emission layers, with POS spatial correlations



$$B = \underbrace{B_0}_{\text{Uniform field}} + \underbrace{B_t}_{\text{Turbulent field}}$$

Turbulent-to-mean ratio  $f_M = \frac{\sigma_B}{B_0}$

Spectral index of the turbulent component  $C_\ell \propto \ell^{\alpha_M}$

Molecular clouds  $f_M = 0.5 \pm 0.2$

Planck Collaboration Int. XXXV (2016)

Diffuse ISM at high and intermediate latitudes  $f_M = 0.8 \pm 0.2$

Planck Collaboration Int. XXXII (2016)

Southern Galactic cap  $f_M = 0.9 \pm 0.1$

Planck Collaboration Int. XLIV (2016)

$$\alpha_M \in [-2, -3]$$

- Turbulent magnetic field modelled along the LOS, no POS correlation from pixel to pixel

WMAP 23 GHz polarized synchrotron data Miville-Deschênes et al. (2008)

Models of polarized thermal dust emission at 150 GHz O'Dea et al. (2012)

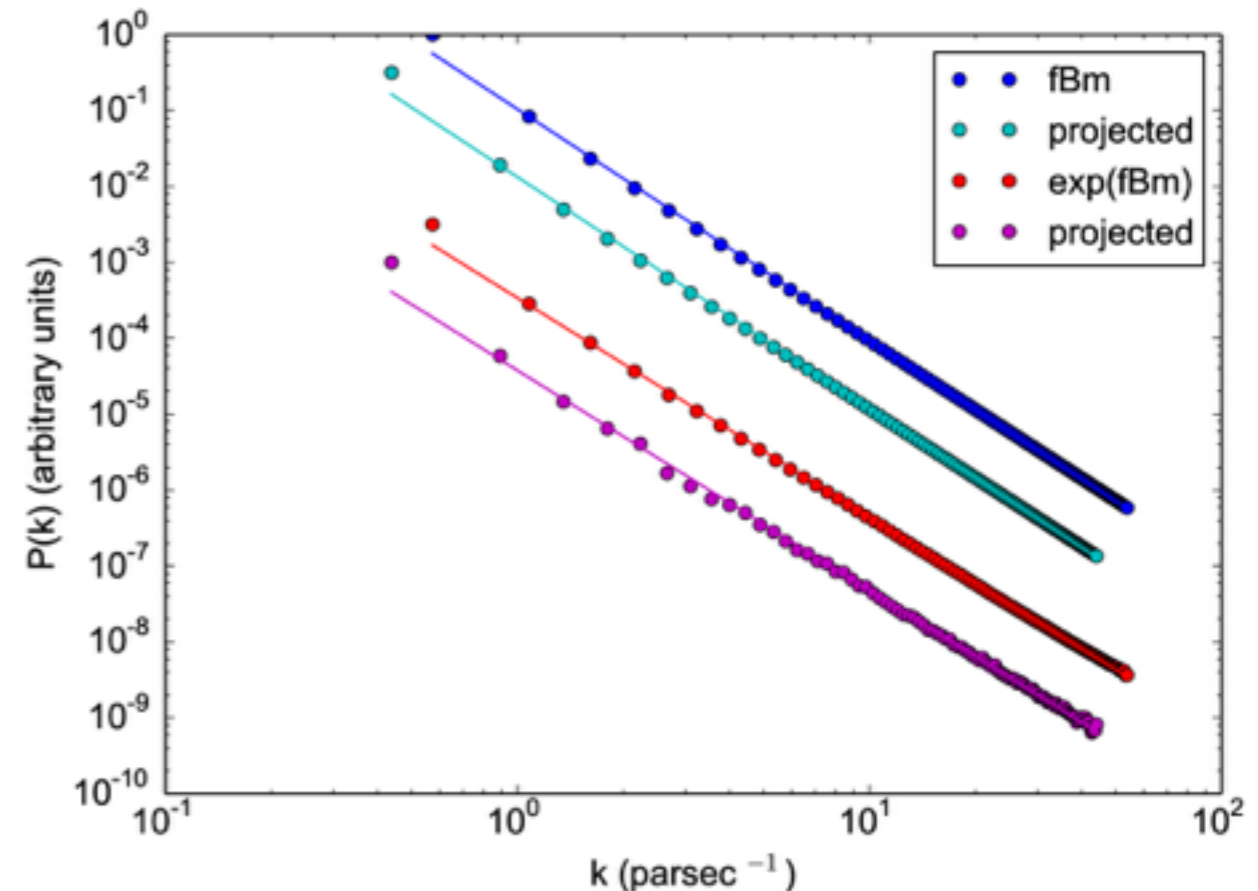
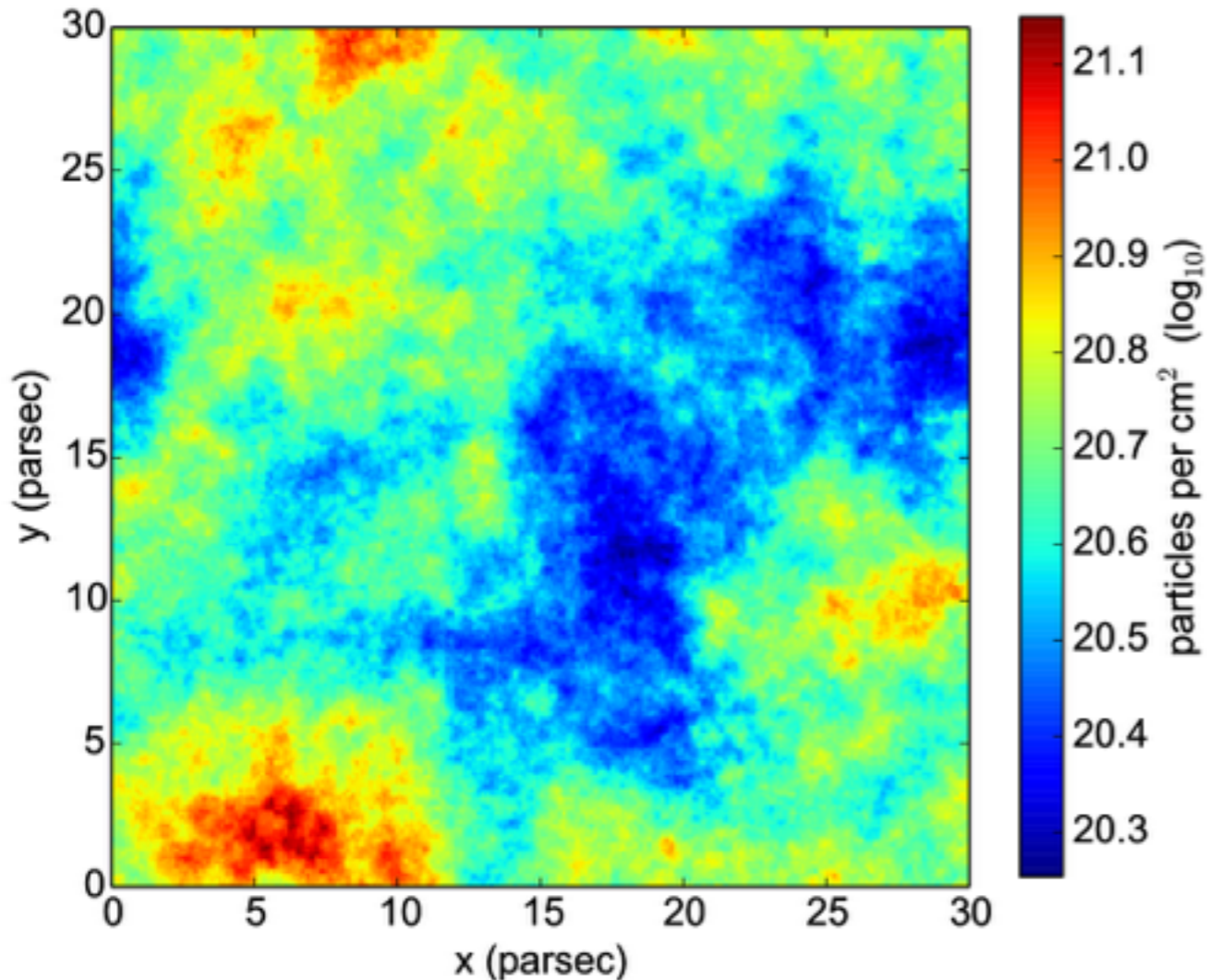
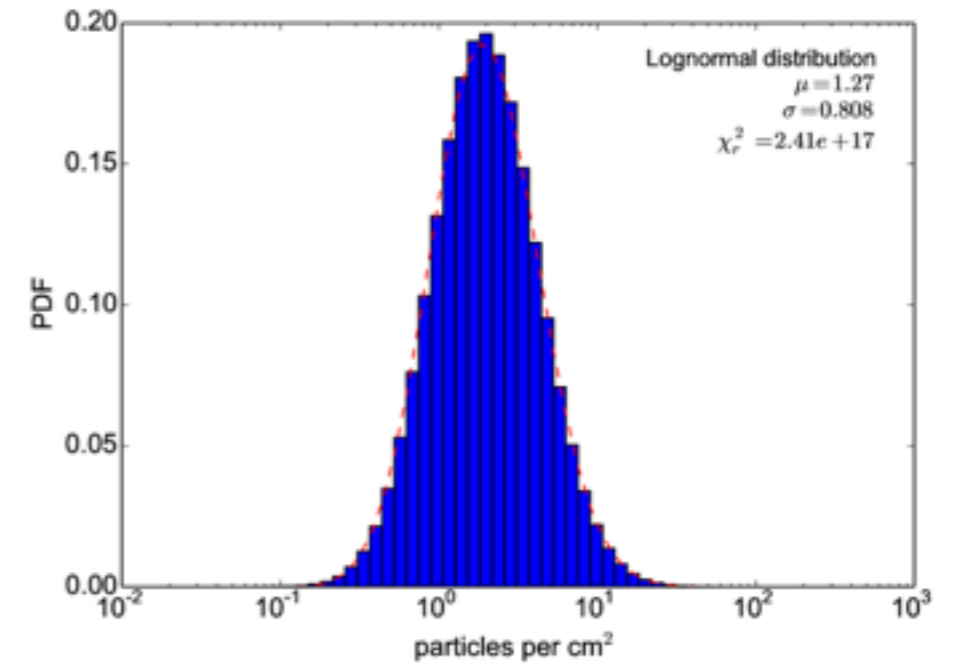
# Modelling polarized thermal dust emission with fBm fields

We wish to constrain the statistical properties of the interstellar B field

**Dust density : exponentiated fractional Brownian motion field (fBm)**

$$n_d = n_0 \exp\left(\frac{X}{X_r}\right)$$

- ▶ Power-law power spectrum with index  $\beta_n$
- ▶ Log-normal distribution
- ▶ Possibly large fluctuations  $\frac{\sigma_n}{n_d} > 0.3$





# Modelling polarized thermal dust emission with fBm fields

Magnetic field from fBm vector potential components

$$\mathbf{B} = \nabla \times \mathbf{A}$$

$$\widetilde{B}_\lambda(\mathbf{k}) = \epsilon_{\lambda\mu\nu} i k_\mu \mathcal{F}_0 |\mathbf{k}|^{-\beta_A/2} \exp[i\phi_{A_\nu}(\mathbf{k})]$$

Input Fourier phase map

Levi-Civita tensor

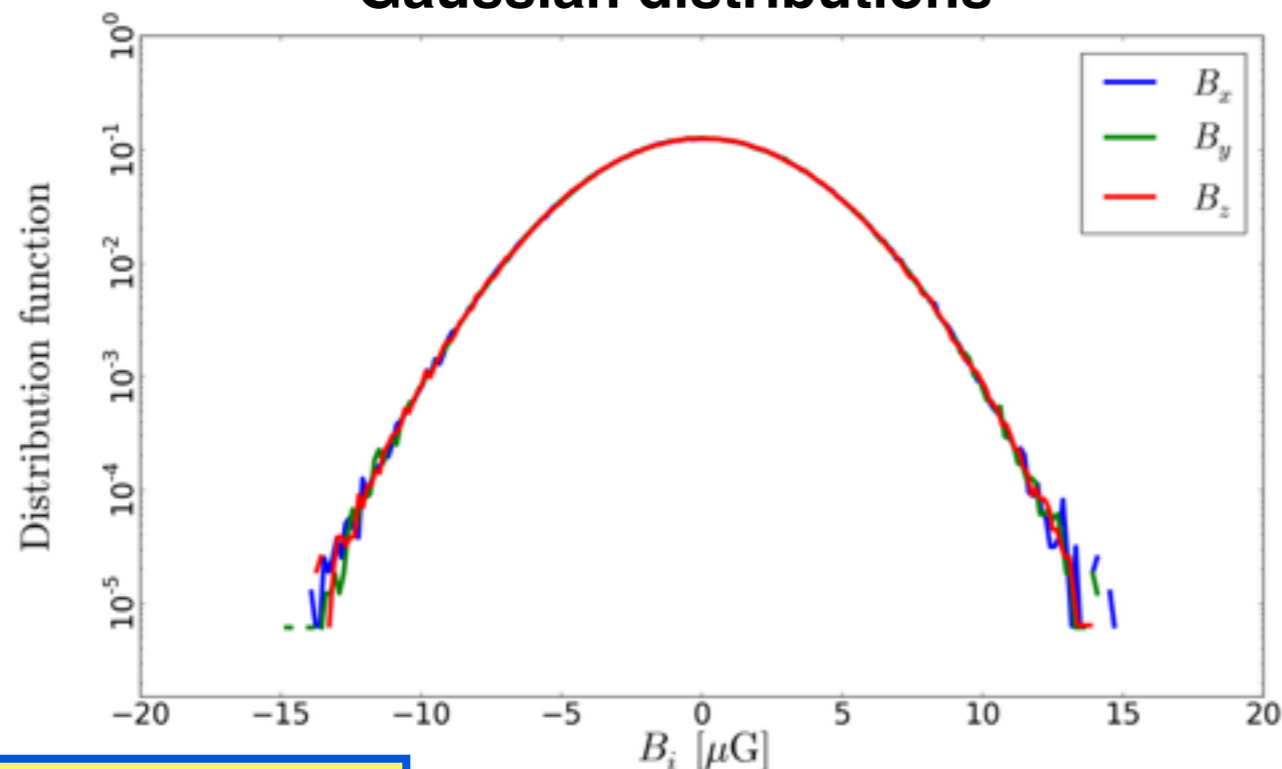
Input spectral index

Component of the B field in Fourier space

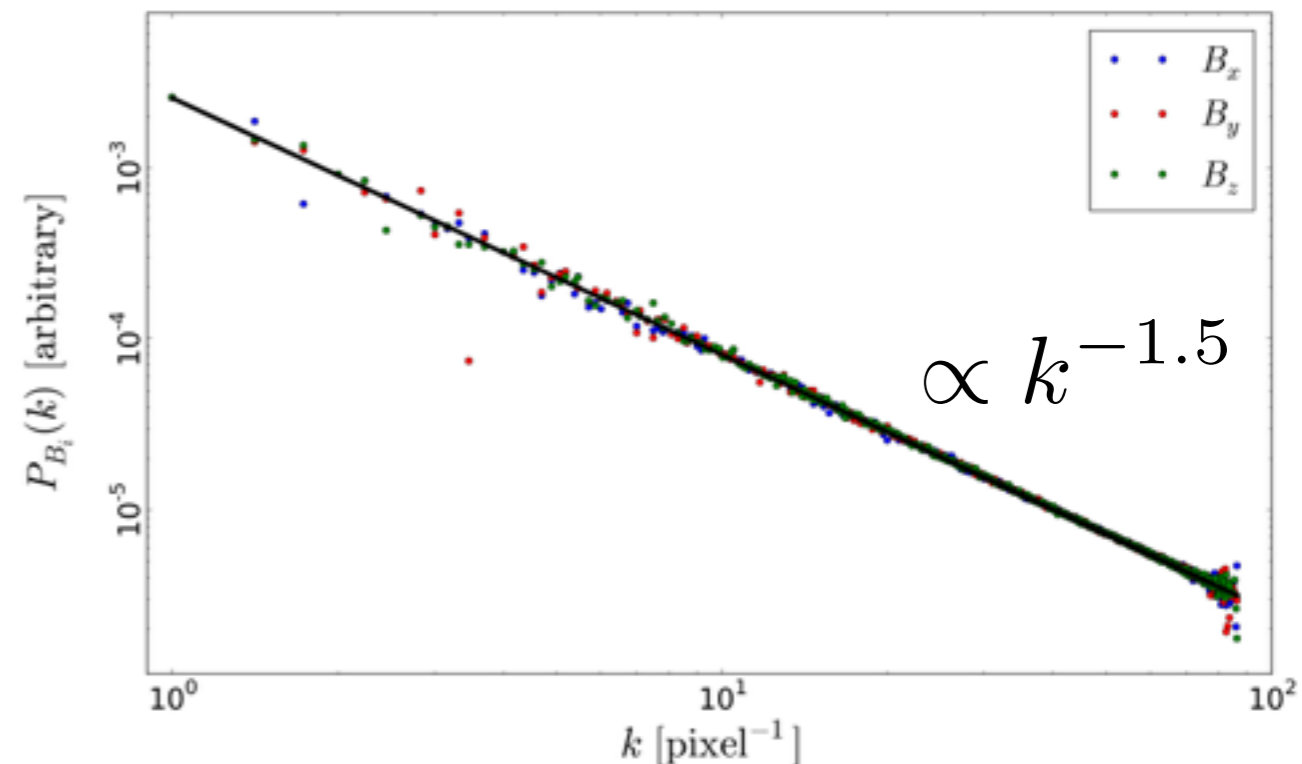
- ▶ Power-law power spectrum with index  $\beta_B = \beta_A - 2$
- ▶ Divergence-free by construction
- ▶ Gaussian distribution with zero mean
- ▶ Possibility to add a large-scale uniform field

$\widetilde{A}_\nu(\mathbf{k})$  fBm fields

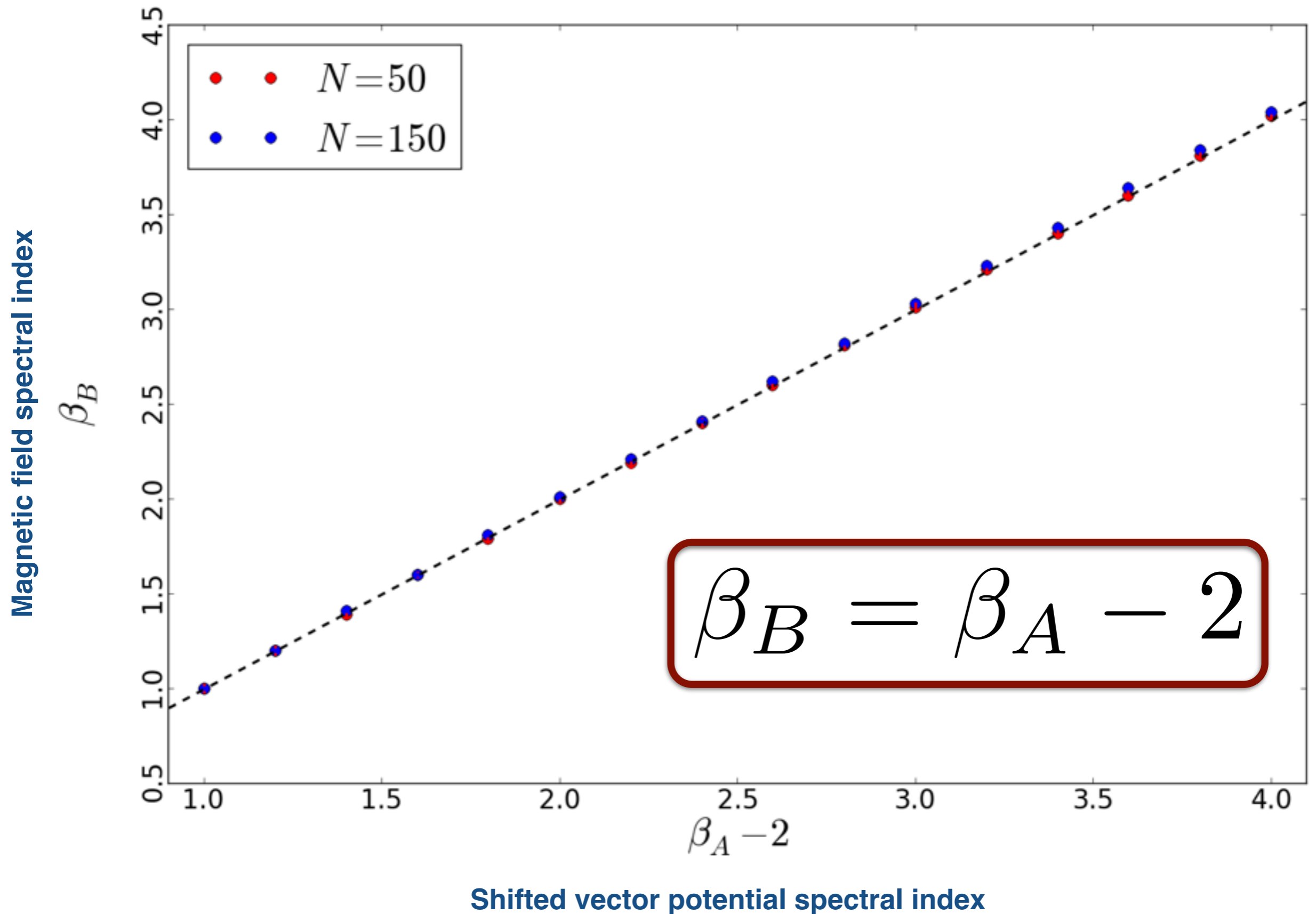
Gaussian distributions



Power-law power spectra



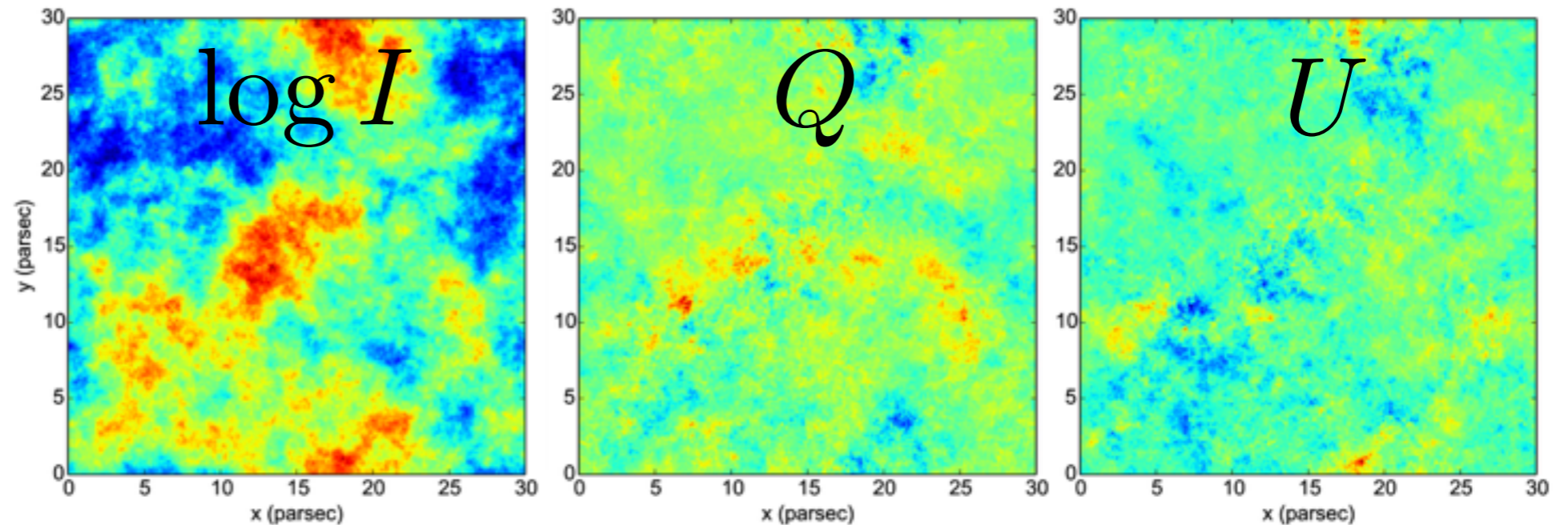
# Synthetic magnetic field spectral index



# Parameter space exploration

- Parameters are spectral indices, fluctuation levels, angle of the mean field and depth on the LOS
- Simulated polarization maps characterized by PDFs, power spectra, and correlations
- Monte-Carlo Markov Chain exploration of parameter likelihood given input polarization maps

Parameter	Prior
$\beta_B$	[1, 4]
$\beta_n$	[1, 5]
$\log_{10} y_n$	[-1, 1]
$\log_{10} y_B^{\text{POS}}$	[-1, 1]
$\chi$	$[-90^\circ, 90^\circ]$
$\log_{10} (d/1 \text{ pc})$	[-0.3, 1.5]

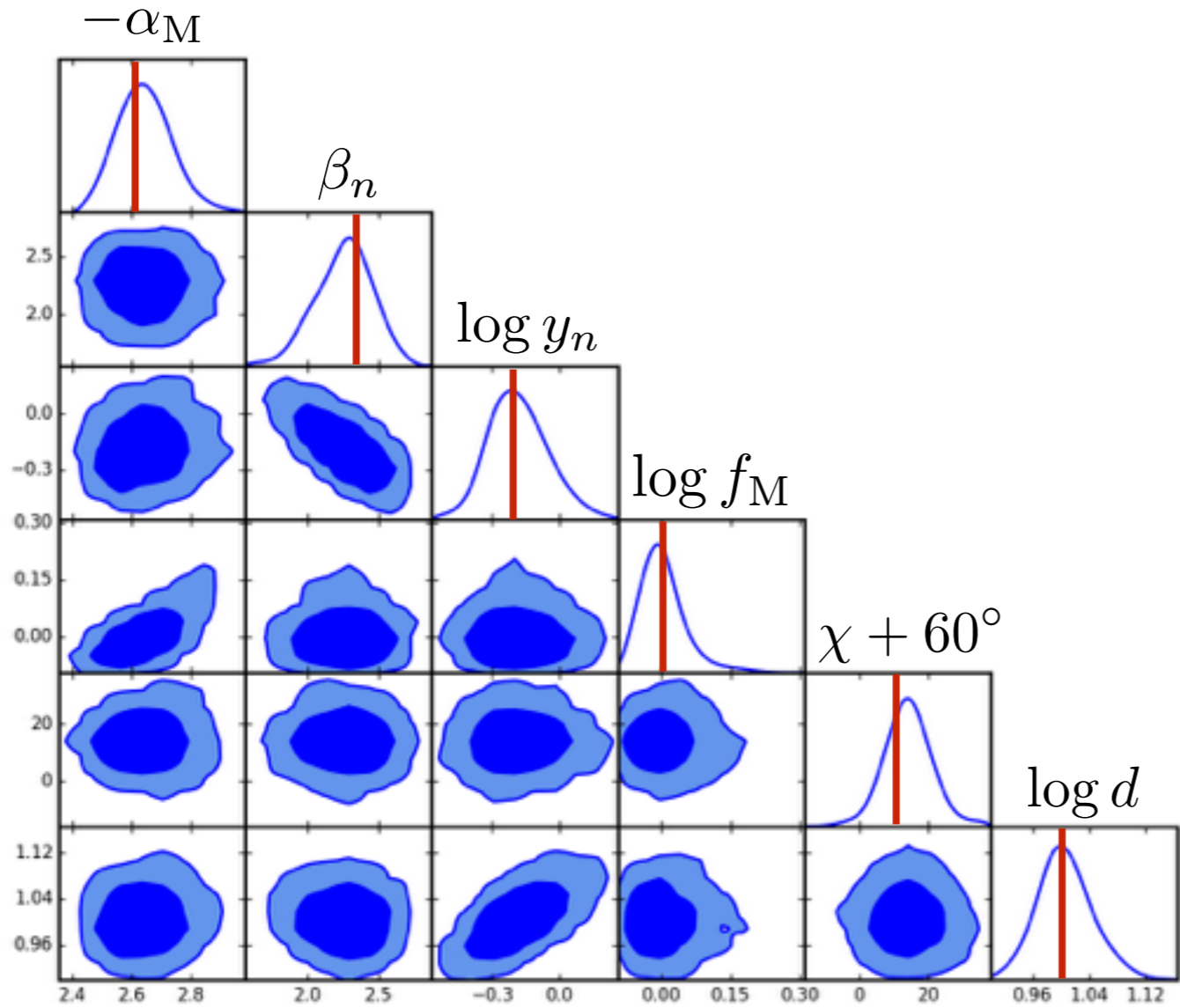


Type	From	Method
PDF	$i, q, u, p_{\text{MAS}}, \psi, \mathcal{S}$	Bin by bin fit of the histogram
Power spectrum	$I_m, Q_m, U_m$	Bin by bin fit of the power spectrum
Correlation	$\{\mathcal{S}, p_{\text{MAS}}\}$	Bin by bin fit of the scatter plot



# Validation of the method

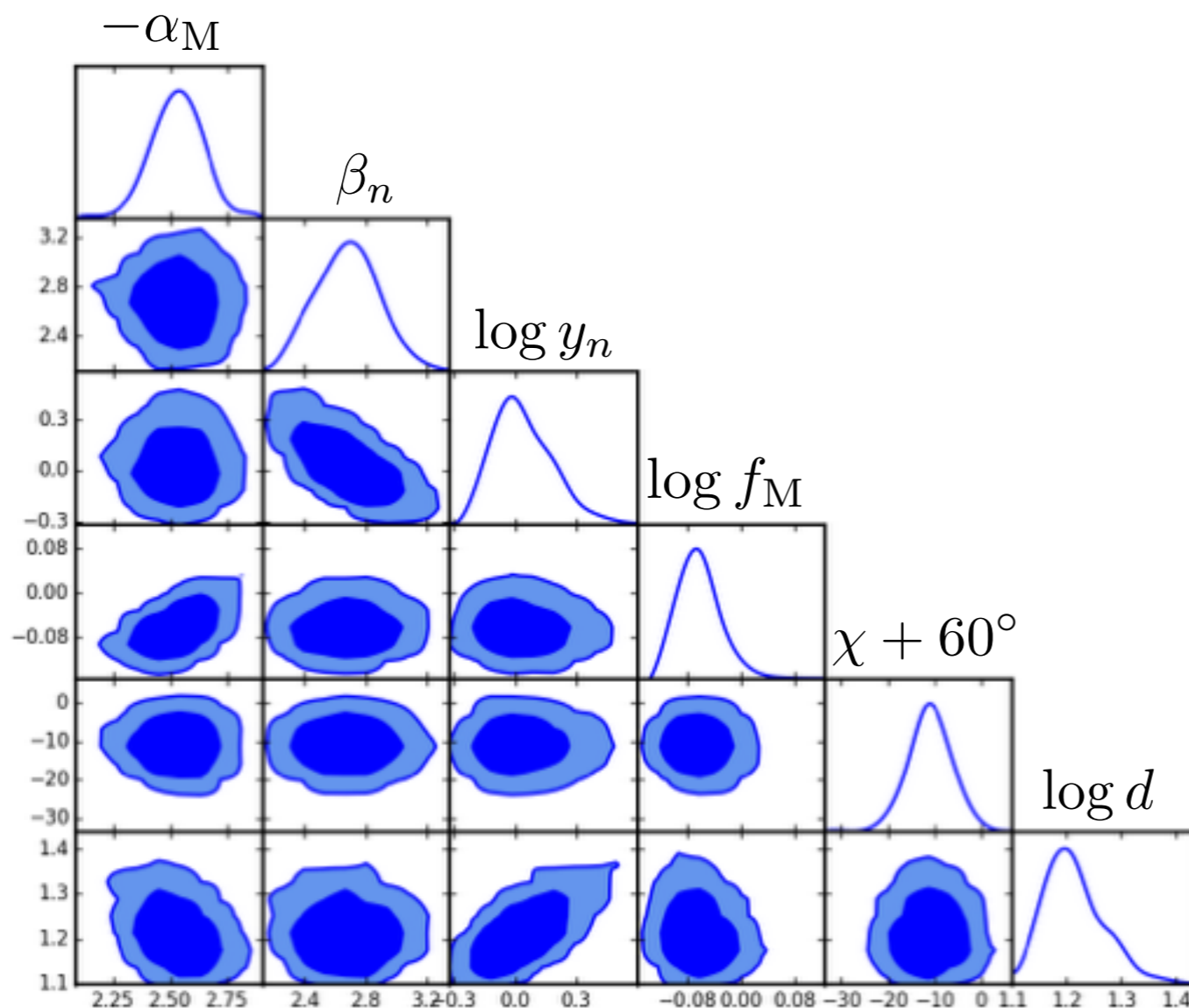
Levrier et al. (in prep)



Parameters	$\beta_B$	$\beta_n$	$\log_{10} y_n$	$\log_{10} y_B$	$\chi$ [°]	$\log_{10} (d/1 \text{ pc})$	$\langle \chi^2_{\text{best}} \rangle$
Simulation D							
Input parameters	2.6	2.31	0.0	-0.05	-70	1.18	
Best fit values	$2.57^{+0.13}_{-0.11}$	$2.45^{+0.46}_{-0.31}$	$-0.02^{+0.14}_{-0.18}$	$-0.02^{+0.03}_{-0.05}$	$-68.6^{+6.1}_{-5.8}$	$1.20^{+0.05}_{-0.06}$	8.7

# Application to Planck data on the Polaris Flare

Levrier et al. (in prep)



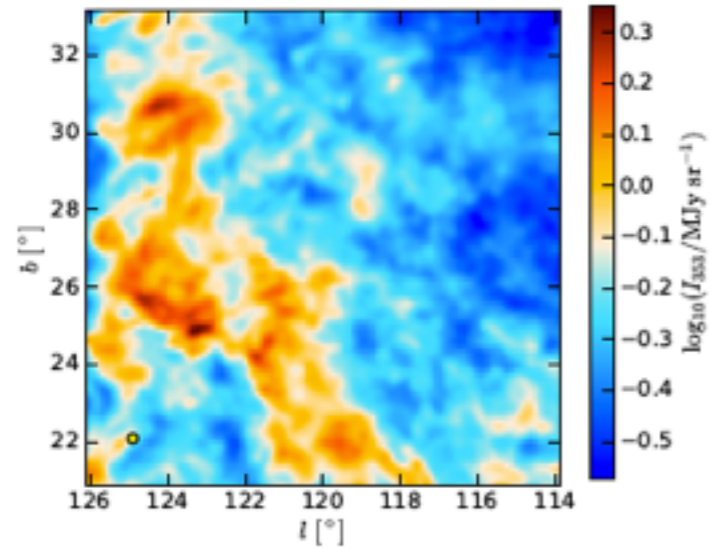
$$\alpha_M = -2.53^{+0.13}_{-0.12}$$

$$f_M = 0.87^{+0.06}_{-0.08}$$

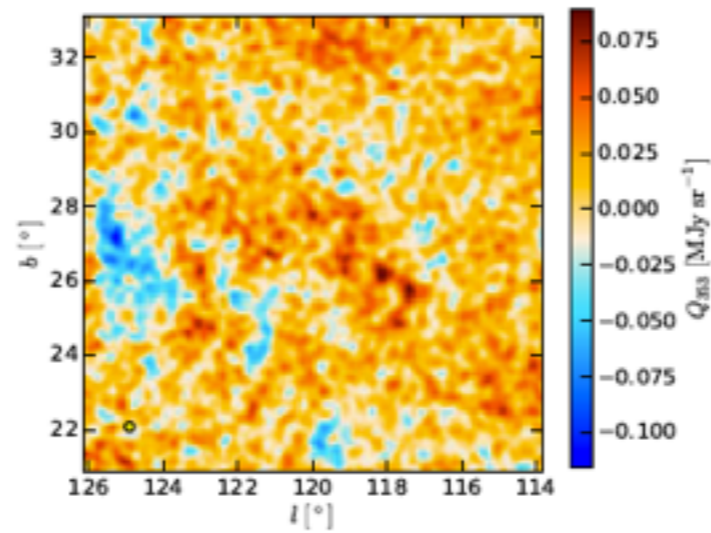
Parameters	$\beta_B$	$\beta_n$	$\log_{10} y_n$	$\log_{10} y_B$	$\chi$ [°]	$\log_{10} (d/1 \text{ pc})$	$\langle \chi^2_{\text{best}} \rangle$
Polaris Flare – no CIB correction							
Best fit values	$2.54^{+0.13}_{-0.13}$	$2.33^{+0.46}_{-0.35}$	$0.04^{+0.15}_{-0.19}$	$-0.06^{+0.03}_{-0.04}$	$-71.3^{+5.4}_{-5.7}$	$1.21^{+0.06}_{-0.07}$	16.3
Polaris Flare – CIB correction							
Best fit values	$2.43^{+0.12}_{-0.12}$	$2.44^{+0.44}_{-0.31}$	$-0.07^{+0.13}_{-0.18}$	$-0.02^{+0.04}_{-0.04}$	$-71.1^{+5.2}_{-5.0}$	$1.19^{+0.06}_{-0.07}$	15.4

# Planck Polaris Flare maps

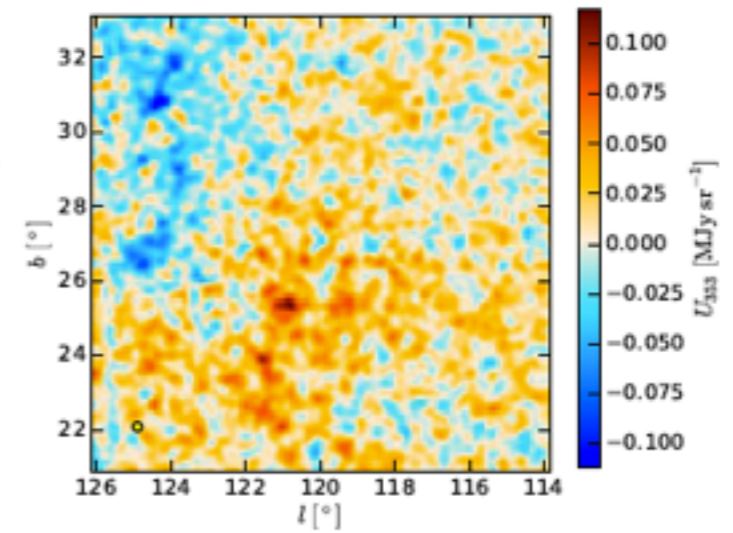
Total intensity



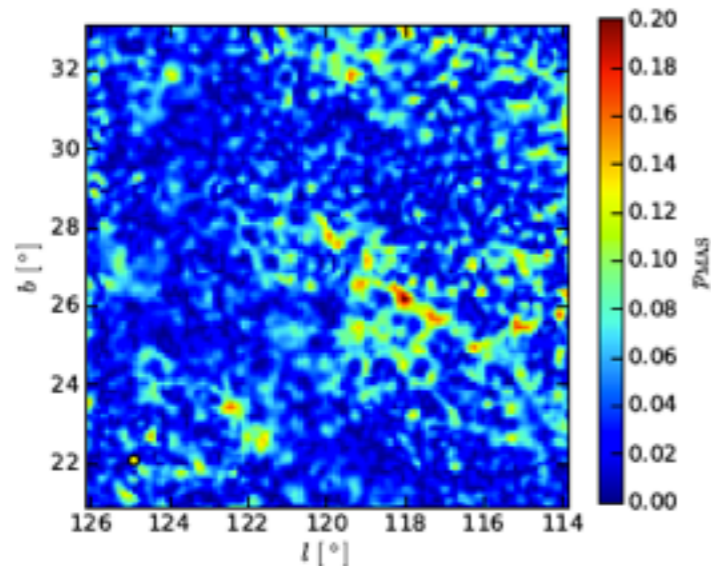
Stokes Q



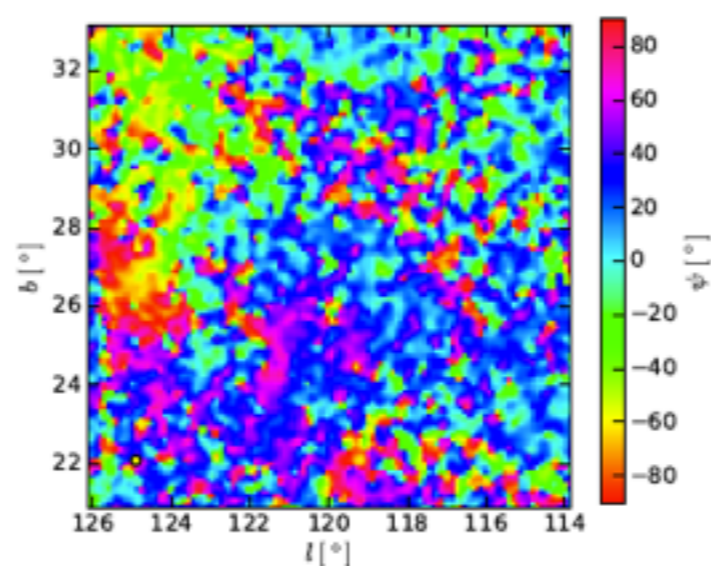
Stokes U



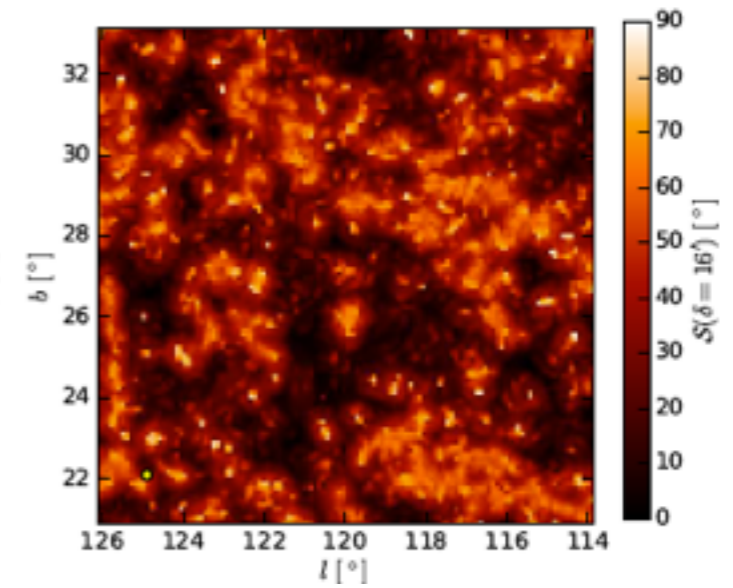
Polarization fraction



Polarization angle

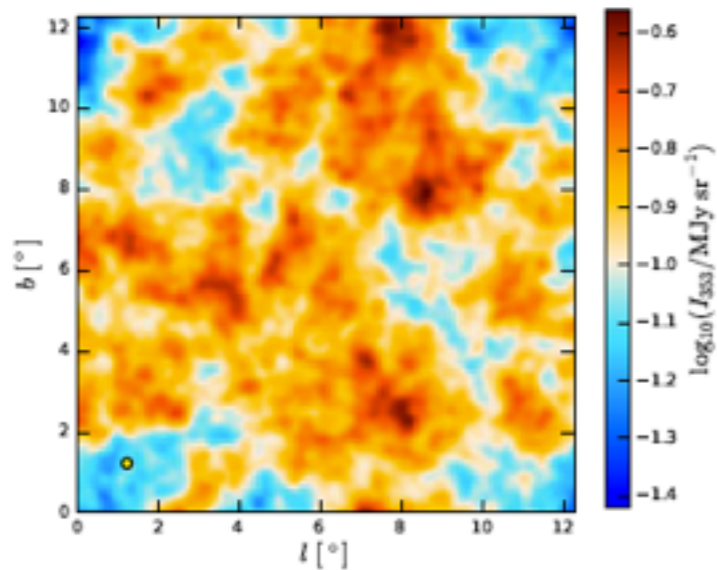


Angular dispersion

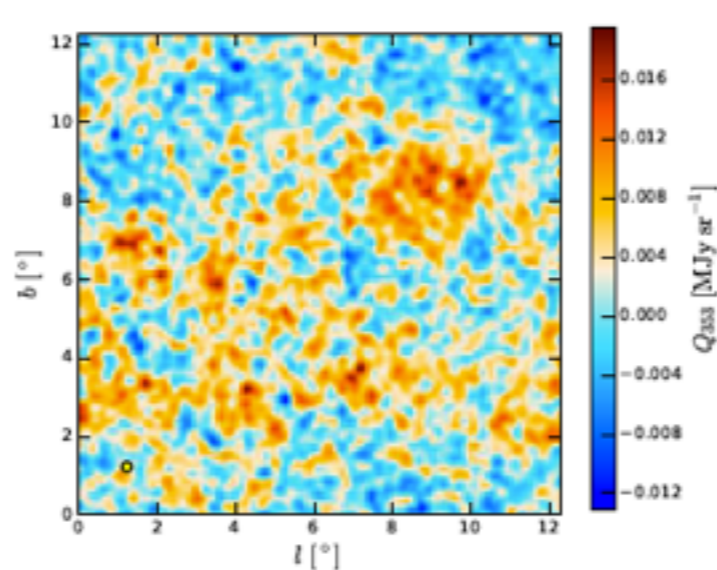


# Simulations maps with best fitting parameters

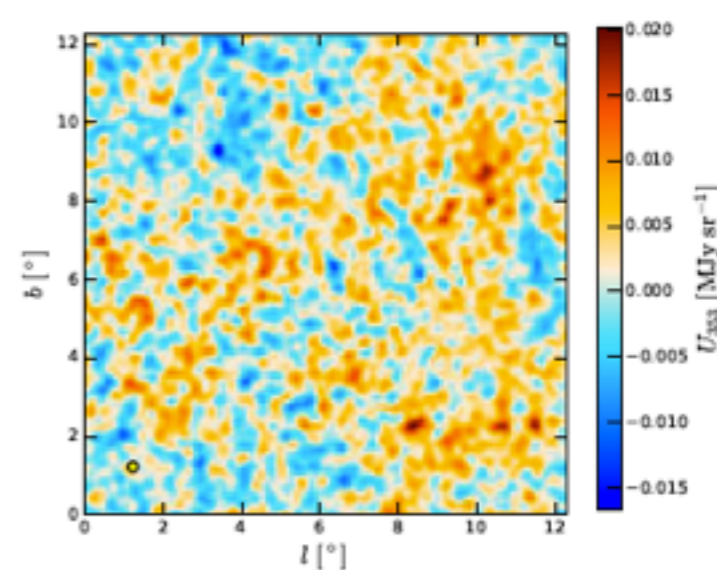
Total intensity



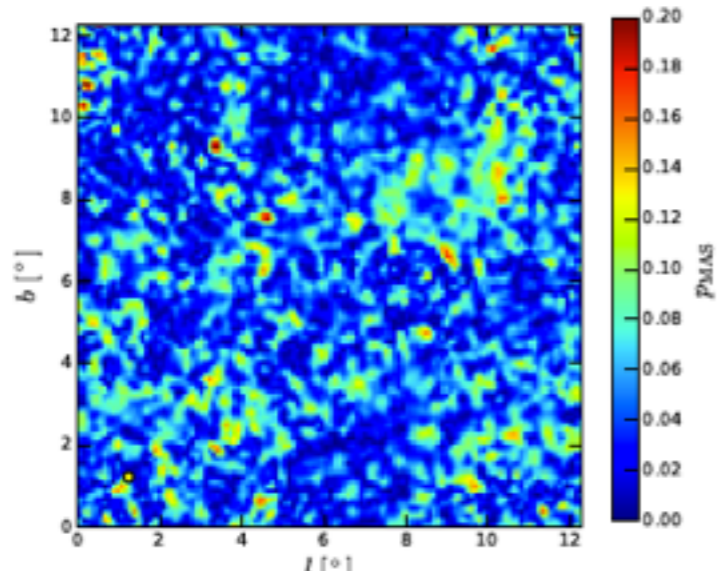
Stokes Q



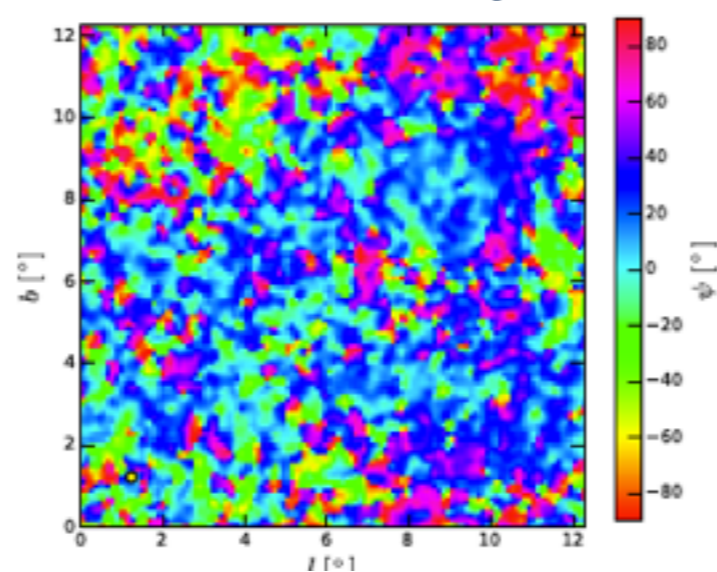
Stokes U



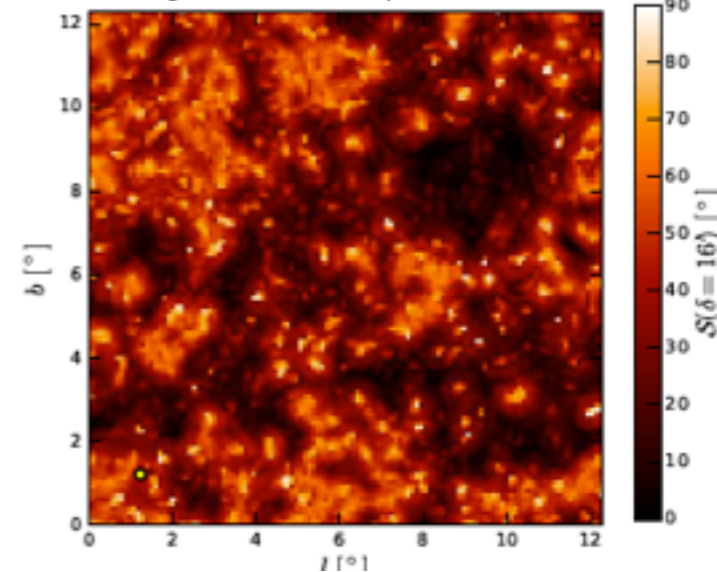
Polarization fraction



Polarization angle

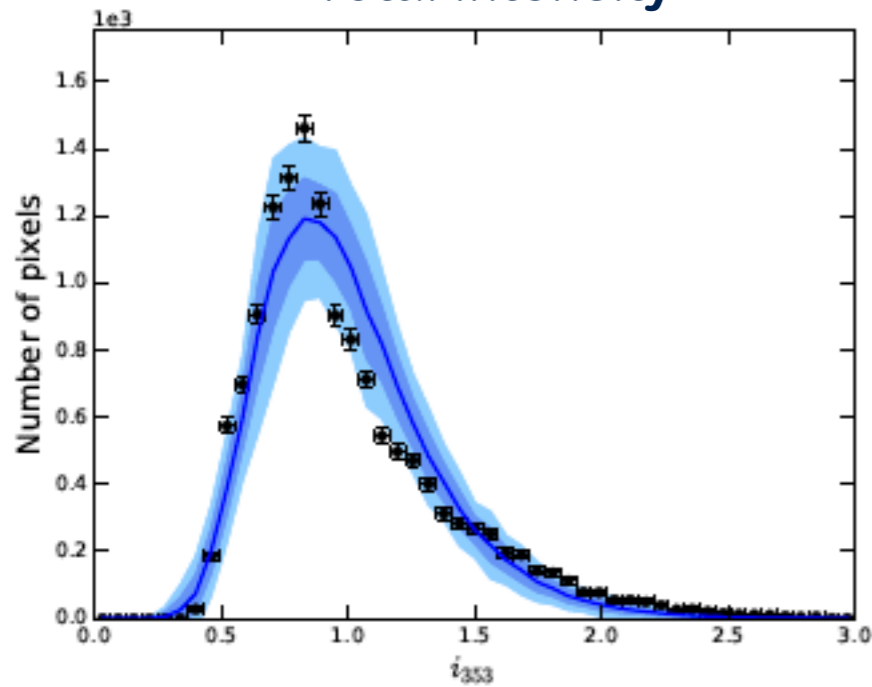


Angular dispersion

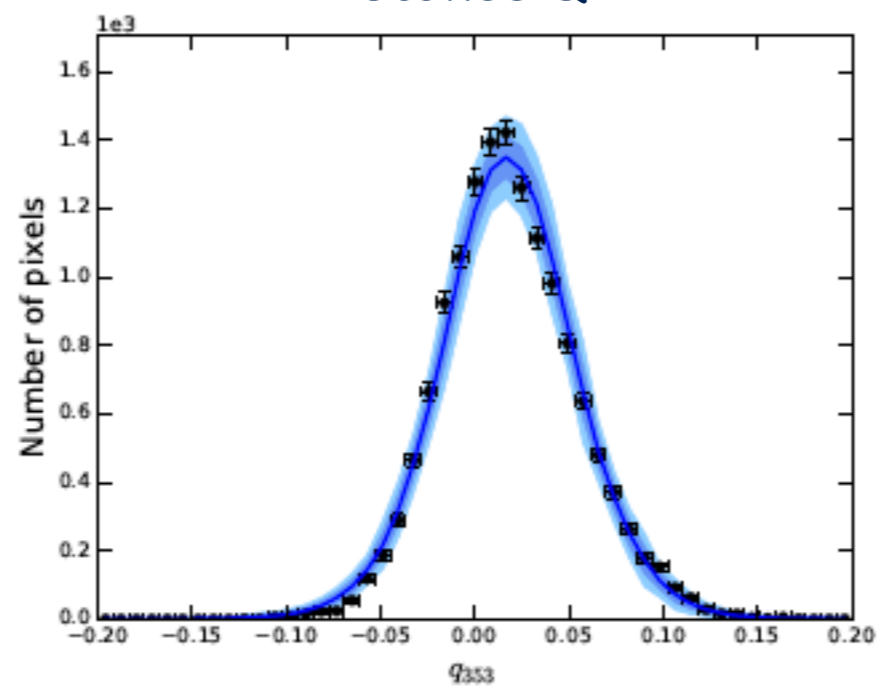


# PDFs of observables (Polaris and best-fit model)

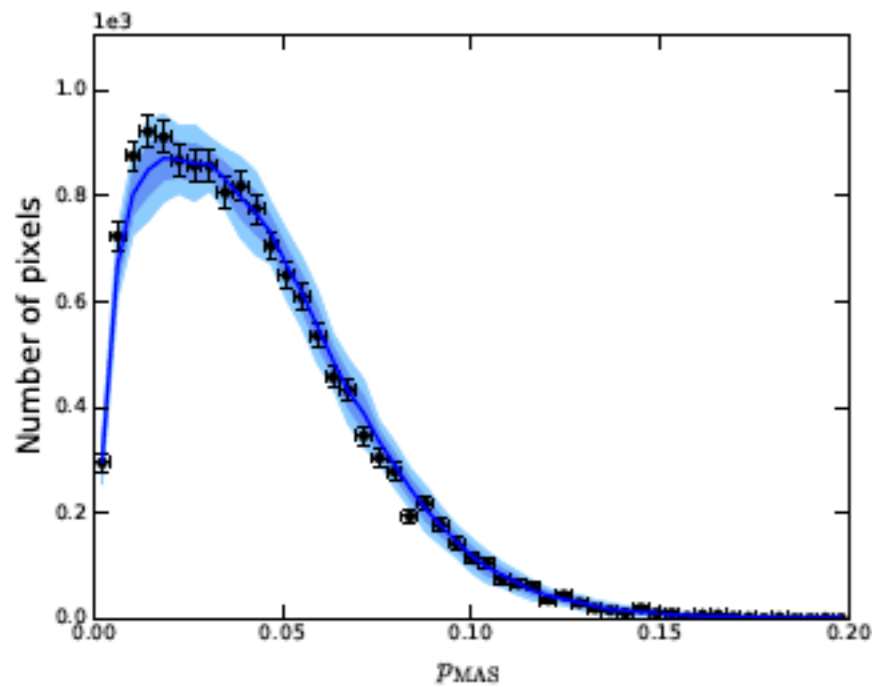
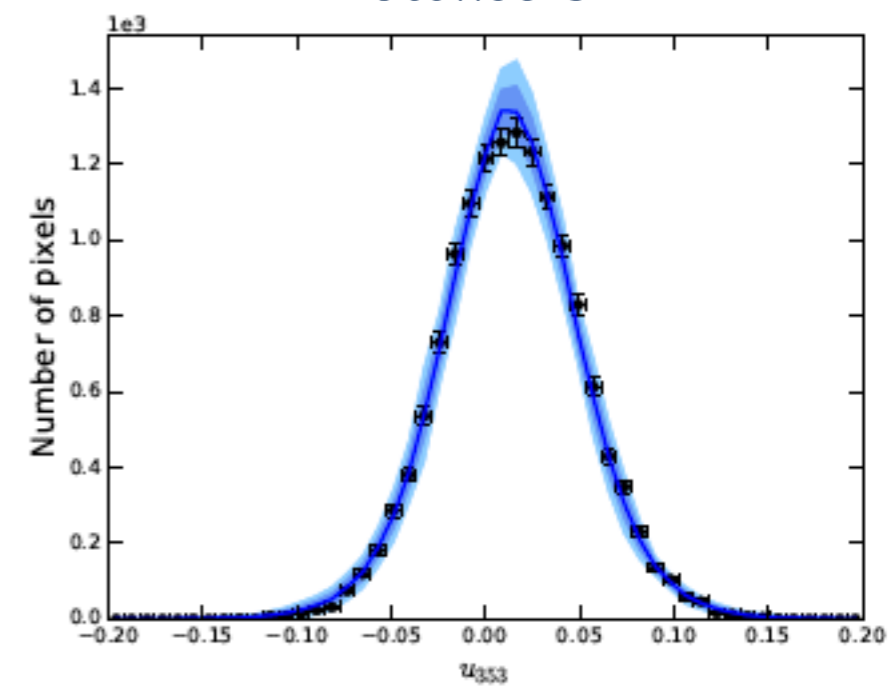
Total intensity



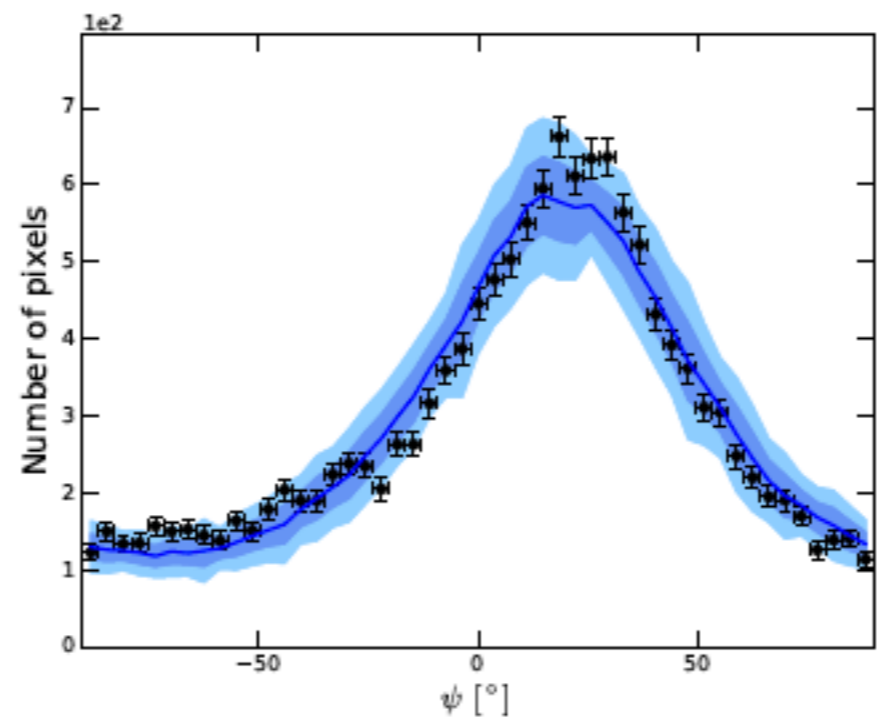
Stokes Q



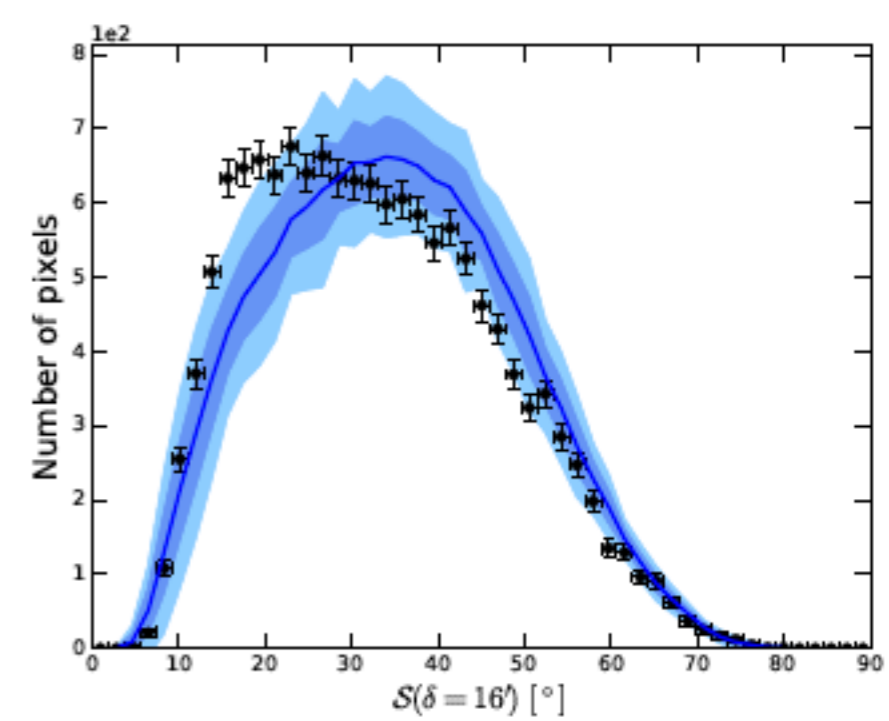
Stokes U



Polarization fraction



Polarization angle

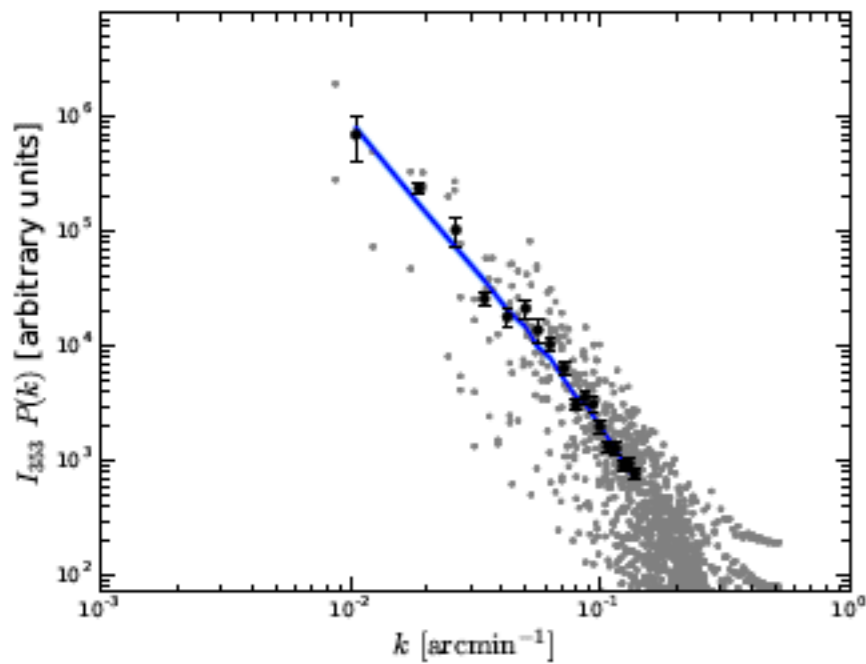


Angular dispersion

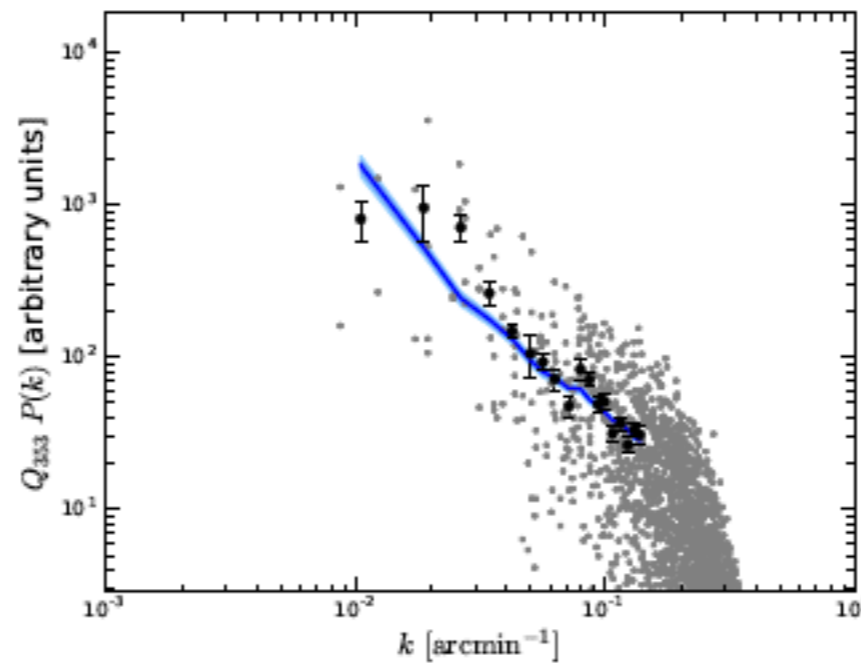


# Power spectra of observables (Polaris and best-fit model)

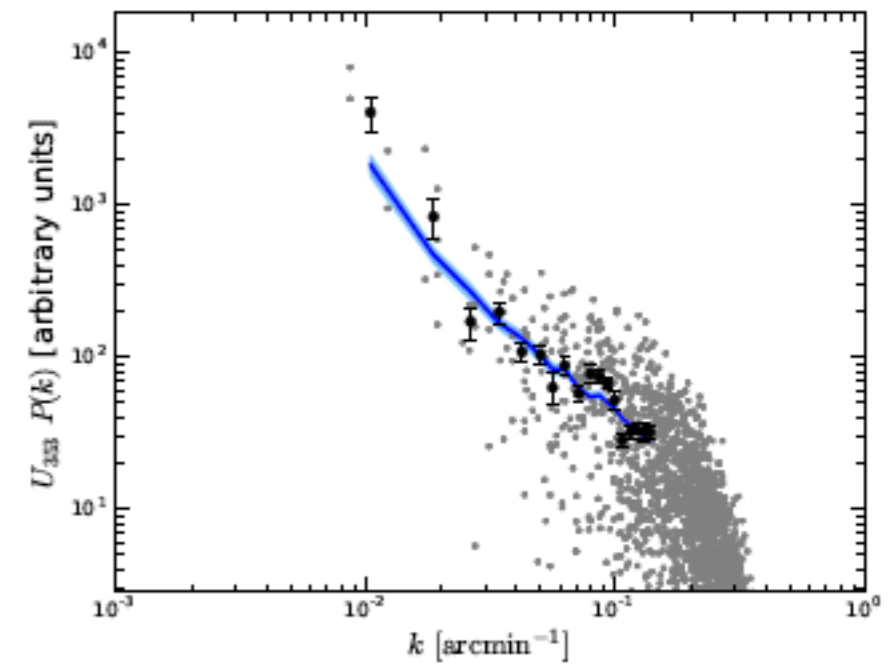
## Total intensity



## Stokes Q

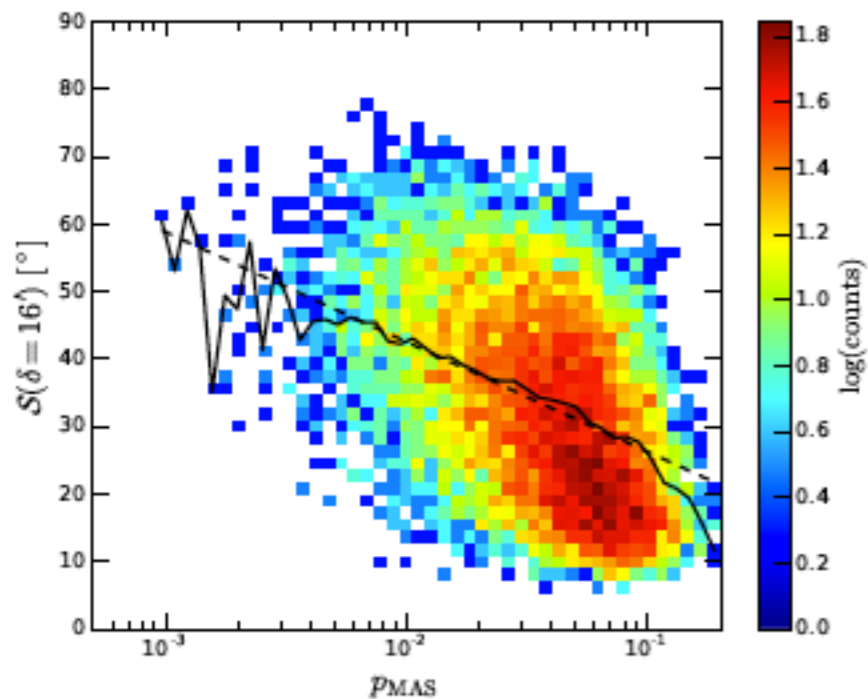


## Stokes U

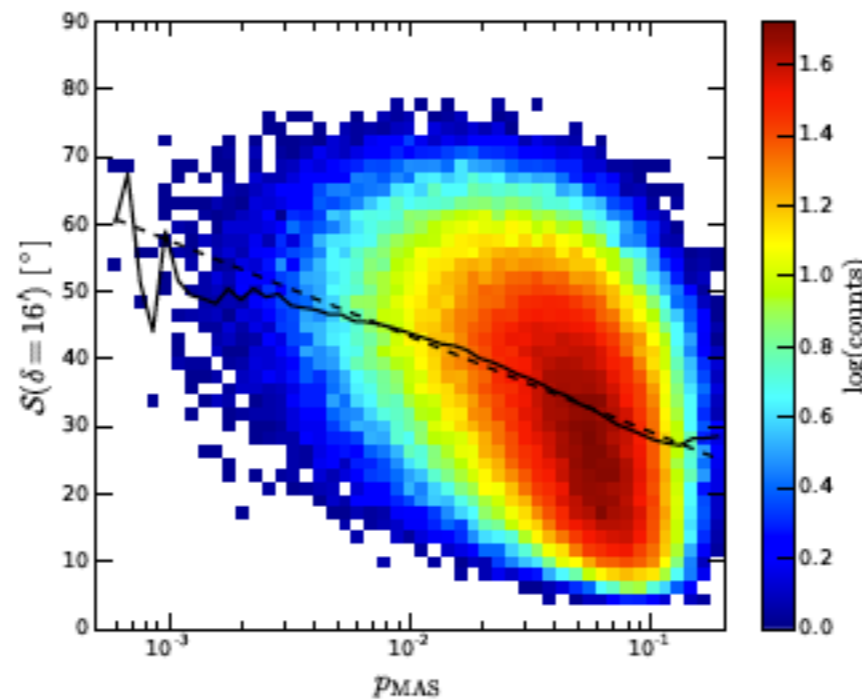


# Correlation polarization fraction - angular dispersion

## Polaris Flare



## Best-fit model



## Residuals

